

BOND FAILURE IN PERIDYNAMICS: NONEQUIVALENCE OF CRITICAL STRETCH AND CRITICAL ENERGY DENSITY CRITERIA

PABLO SELESON*, PABLO RAÚL STINGA*, AND MARY VAUGHAN*

ABSTRACT. This paper rigorously analyzes bond failure in the peridynamic theory of solid mechanics, which is a fundamental component of fracture modeling. We compare analytically and numerically two common bond-failure criteria: *critical stretch* and *critical energy density*. In the former, bonds fail when they stretch to a critical value, whereas in the latter, bonds fail when the bond energy density exceeds a threshold. By focusing the analysis on bond-based models, we prove mathematically that the critical stretch criterion and the critical energy density criterion are not equivalent in general and result in different bond-breaking and fracture phenomena. Numerical examples showcase the striking differences between the effect of the two criteria on crack dynamics, including the crack tip evolution, crack propagation, and crack branching.

1. INTRODUCTION

Modeling material failure and damage is an ongoing challenge in computational science and engineering. Computational solid mechanics has been remarkably successful in the modeling of material behavior, especially based on the finite element method [23]. However, the continuity assumptions of the basic equations of classical continuum mechanics require special techniques to model material discontinuities, such as propagating cracks.

Peridynamics [38, 40] is a nonlocal formulation of classical continuum mechanics, where the mathematical equations are reformulated to accommodate material discontinuities. The nonlocality of peridynamics is expressed in that material points interact with surrounding material points within a finite neighborhood. The connections between them are referred to as *bonds*. Peridynamic governing equations replace spatial differential operators with integral operators that do not require differentiability assumptions, thus allowing the representation of material separation. Connections between peridynamics and classical theory have been established. For elastic materials, peridynamics was shown to converge to classical elasticity under suitable differentiability assumptions as nonlocality vanishes [41], and a link between peridynamics and classical linear elastic fracture mechanics was presented in [21].

To model material separation, such as fracture, peridynamics introduces the concept of *bond failure*, which means that a bond is no longer able to transfer forces between points. This occurs when the bond reaches or exceeds the threshold defined by the failure criterion, which results in bond breaking. It is common to assume that bonds break irreversibly: once a

2020 *Mathematics Subject Classification.* Primary: 74A70, 74R10, 74A45. Secondary: 45K05, 65R20.

Key words and phrases. Peridynamics, bond failure, bond breaking, crack propagation, fracture.

*Authors are listed alphabetically.

This manuscript has been authored in part by UT-Battelle, LLC, under contract DE-AC05-00OR22725 with the US Department of Energy (DOE). The US government retains and the publisher, by accepting the article for publication, acknowledges that the US government retains a nonexclusive, paid-up, irrevocable, worldwide license to publish or reproduce the published form of this manuscript, or allow others to do so, for US government purposes. DOE will provide public access to these results of federally sponsored research in accordance with the DOE Public Access Plan (<https://www.energy.gov/doe-public-access-plan>).

bond is broken, it remains broken for the remainder of the simulation. The incorporation of bond breaking into peridynamic computations enables the modeling of crack initiation and propagation without the need for an external crack law. Therefore, the choice of bond-failure criterion is essential for properly modeling fracture in peridynamics.

The most commonly used bond-failure criteria in peridynamics are the *critical stretch* [39] and the *critical energy density* [8]. The critical stretch criterion establishes that bonds fail once they stretch to a critical value.¹ The critical energy density criterion, in contrast, states that bonds fail once their energy density exceeds a threshold. The critical value for bond failure for each criterion can be determined by calculating the total energy per unit fracture area of bonds crossing a fracture surface (assuming all those bonds are in their critical failure state) and comparing this quantity to the fracture energy; see Sections 3.1 and 4.1 for calculations in three and two dimensions, respectively. Because one criterion relies on bond stretch and the other relies on bond energy density, the question of which criterion should be implemented into a model naturally arises.

In this paper, we meticulously investigate the analytical differences between the critical stretch and critical energy density criteria and present numerical comparisons. In particular, we prove that the two criteria are not equivalent in general. To the best of the authors' knowledge, this is the first mathematically rigorous comparison of the two criteria to appear in the literature. A numerical comparison between the critical stretch criterion and the critical energy density criterion was presented in [5] for two-dimensional mixed-mode I-II fracture cases, but neither analytical investigations nor deep numerical comparisons between these criteria were studied.

We focus our work on bond-based peridynamics [38] and employ a model for brittle elastic materials based on a generalization of the commonly used prototype microelastic brittle (PMB) material model [39]. The model utilizes a material-dependent influence function $\omega(r)$ that depends only on the bond length $r > 0$ and helps determine how much each bond contributes to the peridynamic internal force density. Moreover, we consider both two- and three-dimensional peridynamic formulations. Details on the model are presented in Section 2.

We recast the critical energy density criterion as a critical stretch criterion with a bond-dependent critical stretch; see Lemmas 3.1 and 4.2 for three- and two-dimensional formulations, respectively. This enables direct comparison between the two criteria via the corresponding critical stretch expressions and leads to our main results, Theorems 3.3 and 4.4. Here is an informal version of those results.

Theorem 1.1. *In the generalized PMB model, the critical stretch criterion and the critical energy density criterion coincide if and only if the influence function is $\omega(r) = \beta r^{-1}$ for some $\beta > 0$.*

In particular, we prove that the two criteria are *not* equivalent in general. This includes the original PMB model for which $\omega(r) \equiv 1$ [39]. Indeed, the *only* case in which they are equivalent is when the influence function is exactly $\omega(r) = \beta r^{-1}$ for some $\beta > 0$.

Remarkably, when they are not equivalent, the two criteria yield different bond-breaking and fracture behaviors. As an illustrative example, we consider influence functions given by

$$(1.1) \quad \omega(r) = r^{-\alpha} \quad \text{for some } \alpha < d + 1,$$

where $d = 2, 3$ is the spatial dimension. We show analytically that the choices of bond-failure criterion and of influence function dictate if either shorter or longer bonds will break first; see

¹In [39], bonds remain unbroken as long as their stretch is below the critical stretch, implying that a bond breaks once it reaches this limit. However, in later works, the critical stretch criterion often assumes that bonds break once their stretch exceeds this limit.

Theorem 3.4 for the three-dimensional case and Theorem 4.5 for the two-dimensional case. We informally write those results here.

Theorem 1.2. *In the generalized PMB model, let $\omega(r) = r^{-\alpha}$ for $\alpha \neq 1$.*

- (1) *Assume that $\alpha < 1$. Shorter bonds that break under the critical stretch criterion may not break under the critical energy density criterion. Longer bonds that break under the critical energy density criterion may not break under the critical stretch criterion.*
- (2) *Assume that $1 < \alpha < d + 1$. Longer bonds that break under the critical stretch criterion may not break under the critical energy density criterion. Shorter bonds that break under the critical energy density criterion may not break under the critical stretch criterion.*

Recasting the critical energy density criterion as a bond-dependent critical stretch criterion also allows for straightforward numerical implementation. We simply modify the expression of the critical stretch in the bond-breaking condition in peridynamics codes that already implement the critical stretch criterion.

We confirm our mathematical results through several numerical experiments on two-dimensional problems, comparing the critical stretch and critical energy density criteria, using influence functions of the form (1.1). First, we consider a simple isotropic extension, which showcases the strikingly different bond-breaking patterns for various influence functions, i.e., for different values of α (see Section 5.1). Then, we illustrate the notably distinct bond-breaking behavior exhibited by the two bond-failure criteria during the evolution of a crack tip for given influence functions (see Section 5.2). Both of these examples substantiate Theorem 1.2. Finally, we study crack propagation and branching, using an example of a pre-notched plate subjected to traction loading as an illustration. Our results confirm that there are undeniable differences when implementing the critical stretch criterion versus the critical energy density criterion. Indeed, taking $\alpha = 2$, for the critical stretch criterion, the crack evolves as a single horizontal line, but for the critical energy density criterion, the crack branches. After increasing the traction, both criteria result in crack branching, but the crack paths are significantly different (see Section 5.3). Taking instead $\alpha = 0$, the different behaviors are apparent but more subtle. For instance, we find that the crack tip propagates slower under the critical stretch criterion than under the critical energy density criterion.

Our analytical results and numerical simulations indicate major implications in modeling that need to be understood. It is not clear a priori which bond-failure criteria should be utilized and thus deeper mathematical and numerical investigations are required.

1.1. Literature review. The original peridynamic formulation was based on pairwise interactions and is referred to as *bond-based peridynamics* [38]. This formulation was later extended to multibody interactions under *state-based peridynamics* [40], which eliminates modeling restrictions imposed by the bond-based formulation such as a fixed Poisson's ratio (see Remark 2.2). As indicated above, we focus on comparing the critical stretch and critical energy density criteria in bond-based peridynamics, a formulation that models the response of a bond independently of the state of other bonds, thus enabling the establishment of single-bond rules for bond breaking for both criteria.

Variations of the critical stretch and critical energy density criteria exist in the literature. The commonly used critical stretch criterion assumes that the critical stretch of a given bond is independent of the state of other bonds. A generalization was presented in [39], in which the critical stretch depends on the minimum stretch among all bonds connected to a given point. Moreover, while the critical stretch criterion was initially proposed for a bond-based model, derivations of a critical stretch for a state-based model were presented in [1, 26, 50], and

various approaches for incorporating critical stretch-based bond failure within a state-based model were discussed in [18]. To account for material anisotropy, an orientation-dependent critical stretch criterion was presented in [11] for the modeling of orthotropic media, with applications to unidirectional fiber-reinforced composites, cortical bone, and polycrystalline microstructures. This criterion was also employed in [31] for the modeling of fiber-reinforced composite laminates, and a similar approach was discussed in [32]. Furthermore, a critical energy density criterion, similar to the one proposed in [8] but based on the J -integral, was presented in [25] with applications involving plasticity.

For mathematical analysis, continuous damage formulations were proposed that enable the weakening of bond forces without resulting in immediate bond breaking. A modified critical stretch criterion that incorporates partial bond failure through linear bond degradation was proposed for a bond-based model in [7], and a similar approach was presented in [6]. A bond-based model with softening behavior, but without irreversible bond breaking, was presented in [20]. This softening approach was extended to a state-based model that enables irreversible damage in [22]. State-based models extending those from [6] and [22] were presented in [1] with a focus on applications rather than on mathematical analysis; these models are related to one of the approaches discussed in [18].

Other bond-failure criteria have also been proposed. For example, several works featured the critical shear angle criterion, which is based on bond rotation. This criterion was used for Mode II (in-plane shear) fracture analysis in [49] (where it is referred to as the critical skew criterion) and for Mode III (anti-plane shear) and torsional fracture analysis in [29]. To model fiber-reinforced composites, [28] combined the critical stretch criterion for normal interlayer bonds with the critical shear angle criterion for shear bonds to simulate the interaction between neighboring plies in a laminate, thereby enabling Mode I (tensile) and Mode II failure, respectively. To distinguish tensile cracks from shear cracks in mixed-mode I-II fracture analysis of rock-like materials, the critical stretch and critical shear angle criteria were augmented, respectively, with dilatational and deviatoric deformation information in [46]. In [45], a conjugated bond-pair-based peridynamic model was presented that uses the critical stretch criterion for Mode I failure and the critical bond shear energy density criterion for Mode II and III failure. A combined bond-failure criterion was presented in [24], under which a bond fails if it satisfies either the critical stretch criterion or the critical shear angle criterion. A similar concept, but based on the bond strain energy density, was presented in [19]: a bond fails if the strain energy density associated with its normal or tangential deformations exceeds a threshold. An approach that compensates the critical energy density criterion with the critical shear angle criterion, to account for shear bonds that might otherwise be overlooked, was presented in [48]. Bond failure based on a critical angle between bond pairs was used in [27] for a peridynamic Euler–Bernoulli beam model. In the context of micropolar peridynamics [9], bond-failure criteria based on (tensile and compressive) critical stretch, critical shear angle, and (tensile and compressive) frictional sliding were discussed in [3]. To account for both tensile and shear damage, the critical deviatoric bond strain criterion was introduced in [33].

Bond-failure criteria that incorporate classical concepts of stress or strain have also been proposed. Criteria based on strain invariants—the equivalent strain (which measures the shearing strain) and the average volumetric strain—were discussed in [47]. Stress-based criteria appeared in several works, as follows. The maximum principal stress criterion for tensile failure and the Mohr–Coulomb failure criterion for shear failure were presented in [51]. The maximum principal stress criterion for tensile failure and the twin shear strength criterion for shear failure were employed in [37]. The maximum and minimum principal stress criteria

for tensile and compressive failure, respectively, were applied in [4]. Other proposed stress-based criteria include the Tsai-Hill criterion [13], the incubation time criterion [14, 16, 17], the mean stress criterion [17], and the remote stress criterion [15]. An approach combining a stress-based failure criterion with a bond-failure criterion was proposed in [42]: the model checks whether the stress-based condition is met at a point before assessing the bond-failure condition for bonds connected to that point. Some of the approaches described in this paragraph were presented within the peridynamic correspondence modeling framework; this framework enables the direct incorporation of classical continuum mechanics constitutive models in peridynamics [40]. An approach to integrate classical continuum damage laws within the peridynamic correspondence modeling framework was presented in [44] by modifying the influence function based on the state of accumulated damage, demonstrated using the Johnson–Cook damage model for ductile damage in metals.

Despite the wide variety of bond-failure criteria put forward in the literature, the critical stretch and critical energy density criteria remain the most broadly used approaches in peridynamic fracture simulations and thus constitute the focus of our analysis.

1.2. Organization of the paper. The organization of this paper is as follows. In Section 2, we review the bond-based peridynamic formulation and a brittle elastic material model for two- and three-dimensional problems. In Sections 3 and 4, for three- and two-dimensional problems respectively, we discuss the critical stretch and critical energy density criteria and present our main results: Theorems 3.3 and 4.4. In Section 5, we present a numerical comparison between the two bond-failure criteria with various examples. A summarizing discussion is presented in Section 6.

2. BOND-BASED PERIDYNAMIC MODEL FOR GENERALIZED PMB MATERIALS

We consider two- and three-dimensional peridynamics problems. For the three-dimensional formulation, we let $\Omega \subset \mathbb{R}^3$ be a bounded domain. For the two-dimensional formulation, we still work in three spatial dimensions and consider a plane stress or plane strain body of thickness h in the out-of-plane direction, represented by a two-dimensional domain $\Omega \subset \mathbb{R}^2$. We will refer to these as 3D and 2D problems, respectively.

Let $\mathbf{u}(\mathbf{x}, t)$ denote the displacement of a point $\mathbf{x} \in \Omega$ at time t . The bond-based peridynamic equation of motion introduced in [38] is

$$(2.1) \quad \rho \ddot{\mathbf{u}}(\mathbf{x}, t) = \int_{\mathcal{H}_{\mathbf{x}}} \mathbf{f}(\mathbf{u}(\mathbf{x}', t) - \mathbf{u}(\mathbf{x}, t), \mathbf{x}', \mathbf{x}, t) dV_{\mathbf{x}'} + \mathbf{b}(\mathbf{x}, t),$$

for the three-dimensional case, and

$$(2.2) \quad \rho \ddot{\mathbf{u}}(\mathbf{x}, t) = h \int_{\mathcal{H}_{\mathbf{x}}} \mathbf{f}(\mathbf{u}(\mathbf{x}', t) - \mathbf{u}(\mathbf{x}, t), \mathbf{x}', \mathbf{x}, t) dA_{\mathbf{x}'} + \mathbf{b}(\mathbf{x}, t),$$

for the two-dimensional case (see [36]), where ρ is the mass density, $\ddot{\mathbf{u}}$ is the second derivative of \mathbf{u} with respect to time, i.e., the acceleration, $\mathcal{H}_{\mathbf{x}}$ is a neighborhood of \mathbf{x} , \mathbf{f} is the pairwise force function (with units of force per volume squared), and \mathbf{b} is a prescribed body force density. We assume that

$$\mathcal{H}_{\mathbf{x}} = \{\mathbf{x}' \in \Omega : \|\mathbf{x}' - \mathbf{x}\| \leq \delta\},$$

where $\delta > 0$ is the peridynamic horizon and $\|\cdot\|$ denotes the Euclidean norm. We deal only with homogeneous bodies, but it is necessary to indicate separate dependence on \mathbf{x} , \mathbf{x}' , and t in the pairwise force function in (2.1) and (2.2) to account for bond failure.

As is customary, we denote the relative position vector in the reference configuration and the relative displacement vector, respectively, by

$$\boldsymbol{\xi} := \mathbf{x}' - \mathbf{x} \quad \text{and} \quad \boldsymbol{\eta} := \mathbf{u}(\mathbf{x}', t) - \mathbf{u}(\mathbf{x}, t).$$

The vector $\boldsymbol{\xi}$ is also known as the *bond*. With this, we can write $\mathbf{f} = \mathbf{f}(\boldsymbol{\eta}, \mathbf{x}', \mathbf{x}, t)$ in the new variables. The following additional restrictions on \mathbf{f} are based on linear and angular momentum [38]:

$$\mathbf{f}(-\boldsymbol{\eta}, \mathbf{x}, \mathbf{x}', t) = -\mathbf{f}(\boldsymbol{\eta}, \mathbf{x}', \mathbf{x}, t) \quad \text{and} \quad (\boldsymbol{\xi} + \boldsymbol{\eta}) \times \mathbf{f}(\boldsymbol{\eta}, \mathbf{x}', \mathbf{x}, t) = \mathbf{0}$$

for all $\boldsymbol{\eta}, \mathbf{x}', \mathbf{x} \in \mathbb{R}^d$ and $t \geq 0$. Noting that $\boldsymbol{\xi} + \boldsymbol{\eta}$ is the relative position vector in the deformed configuration, the *bond stretch* is a measure of strain defined as

$$(2.3) \quad s(\boldsymbol{\eta}, \boldsymbol{\xi}) := \frac{\|\boldsymbol{\xi} + \boldsymbol{\eta}\| - \|\boldsymbol{\xi}\|}{\|\boldsymbol{\xi}\|}.$$

Remark 2.1 (Isotropic extension). Several times, we will consider a static (i.e., time-independent) problem involving a body under an isotropic extension given by $\mathbf{u}(\mathbf{x}) = \bar{s}\mathbf{x}$ for some $\bar{s} > 0$ constant. This results in the relation $\boldsymbol{\eta} = \bar{s}\boldsymbol{\xi}$ between the bond and its relative displacement as well as a constant stretch, $s(\boldsymbol{\eta}, \boldsymbol{\xi}) = \bar{s}$, for all bonds $\boldsymbol{\xi} \in \mathcal{H} \setminus \{\mathbf{0}\}$, where $\mathcal{H} := \mathcal{H}_0$.

A bond-based peridynamic material is microelastic if there is a scalar-valued function $w = w(\boldsymbol{\eta}, \mathbf{x}', \mathbf{x}, t)$, called the pairwise potential or micropotential, such that

$$\mathbf{f}(\boldsymbol{\eta}, \mathbf{x}', \mathbf{x}, t) = \frac{\partial w}{\partial \boldsymbol{\eta}}(\boldsymbol{\eta}, \mathbf{x}', \mathbf{x}, t).$$

The micropotential $w(\boldsymbol{\eta}, \mathbf{x}', \mathbf{x}, t)$ is the energy density (energy per unit volume squared) stored in the bond at time t . It can be shown that w only depends on $\boldsymbol{\eta}$ through $\|\boldsymbol{\eta} + \boldsymbol{\xi}\|$ and there is a scalar-valued function f such that

$$\mathbf{f}(\boldsymbol{\eta}, \mathbf{x}', \mathbf{x}, t) = f(\boldsymbol{\eta}, \mathbf{x}', \mathbf{x}, t) \frac{\boldsymbol{\xi} + \boldsymbol{\eta}}{\|\boldsymbol{\xi} + \boldsymbol{\eta}\|},$$

see [36, 38]. The macroelastic energy density is given by

$$(2.4) \quad W = W(\mathbf{x}, t) = \frac{1}{2} \int_{\mathcal{H}_{\mathbf{x}}} w(\boldsymbol{\eta}, \mathbf{x}', \mathbf{x}, t) dV_{\mathbf{x}'},$$

for the three-dimensional case, and

$$(2.5) \quad W = W(\mathbf{x}, t) = \frac{1}{2} h \int_{\mathcal{H}_{\mathbf{x}}} w(\boldsymbol{\eta}, \mathbf{x}', \mathbf{x}, t) dA_{\mathbf{x}'},$$

for the two-dimensional case (see [36]).

We will only be concerned with brittle elastic materials described by the generalized prototype microelastic brittle (GPMB) constitutive model introduced in [34, 35] (a generalization of the PMB model in [39]) given by

$$(2.6) \quad f(\boldsymbol{\eta}, \mathbf{x}', \mathbf{x}, t) = \mu(\mathbf{x}', \mathbf{x}, t) c \omega(\|\boldsymbol{\xi}\|) s(\boldsymbol{\eta}, \boldsymbol{\xi}),$$

where c is the micromodulus constant (or bond elastic constant), $\omega = \omega(r) : (0, \delta] \rightarrow [0, \infty)$ is the influence function, s is the bond stretch given in (2.3), and $\mu \in \{0, 1\}$ is a history-dependent, Boolean-valued bond-breaking function. In particular, $\mu(\mathbf{x}', \mathbf{x}, t) = 1$ if the bond is intact for all $0 < \tilde{t} \leq t$ and $\mu(\mathbf{x}', \mathbf{x}, t) = 0$ if the bond broke at some time $\tilde{t} \leq t$ (see (3.1) and (3.2) below). The corresponding micropotential is given by

$$(2.7) \quad w(\boldsymbol{\eta}, \mathbf{x}', \mathbf{x}, t) = \frac{1}{2} \mu(\mathbf{x}', \mathbf{x}, t) c \omega(\|\boldsymbol{\xi}\|) s^2(\boldsymbol{\eta}, \boldsymbol{\xi}) \|\boldsymbol{\xi}\|.$$

We assume $\omega(r) > 0$ for $r \in (0, \delta]$. Note that $\omega \equiv 1$ corresponds to the PMB model in [39].

We will now determine the micromodulus constant c in terms of material properties. For this, we separately consider two- and three-dimensional problems.

Remark 2.2. Bond-based peridynamics is restricted to modeling of materials with a Poisson's ratio of $\nu = \frac{1}{4}$ in three dimensions (see [38]). In two-dimensional problems, bond-based peridynamic models are limited to a Poisson's ratio of $\nu = \frac{1}{4}$ for plain strain and $\nu = \frac{1}{3}$ for plane stress (see [10, 43]).

2.1. Three-dimensional problems. For more details on the following discussion, see [39].

Consider a three-dimensional problem of a body under an isotropic extension, so recalling Remark 2.1, $s(\boldsymbol{\eta}, \boldsymbol{\xi}) = \bar{s}$ is constant for some $\bar{s} > 0$. Assume also that no bonds are broken at time t , so that $\mu \equiv 1$ in (2.7). With the explicit form of w in (2.7), we use spherical coordinates in (2.4) to find

$$W = \frac{c\bar{s}^2}{4} \int_{\mathcal{H}} \omega(\|\boldsymbol{\xi}\|) \|\boldsymbol{\xi}\| dV_{\boldsymbol{\xi}} = c\bar{s}^2 \pi \int_0^\delta \omega(r) r^3 dr,$$

for any point in the bulk of the body (i.e., farther than δ from the domain boundary), where \mathcal{H} is defined in Remark 2.1. On the other hand, the strain energy density in classical linear elasticity for the same isotropic extension is $W^C = 9K\bar{s}^2/2$, where K is the bulk modulus. Assuming $W = W^C$, we get

$$(2.8) \quad c = \frac{9K}{2\pi \int_0^\delta \omega(r) r^3 dr} \quad \text{for a 3D problem.}$$

2.2. Two-dimensional problems. For more details on the following discussion, see [36].

Consider a two-dimensional problem of a body in a state of plane strain or plane stress under an isotropic extension, so recalling Remark 2.1, $s(\boldsymbol{\eta}, \boldsymbol{\xi}) = \bar{s}$ is constant for some $\bar{s} > 0$. As above, but now using polar coordinates in (2.5), we get

$$W = \frac{hc\bar{s}^2}{4} \int_{\mathcal{H}} \omega(\|\boldsymbol{\xi}\|) \|\boldsymbol{\xi}\| dA_{\boldsymbol{\xi}} = \frac{hc\bar{s}^2\pi}{2} \int_0^\delta \omega(r) r^2 dr,$$

for any point in the bulk of the body.

Plane strain. For a body in a state of plane strain and under an isotropic extension given by $\mathbf{u}(\mathbf{x}) = \bar{s}\mathbf{x}$ for some $\bar{s} > 0$, it is known from classical linear elasticity that the strain energy density for materials with a Poisson's ratio of $\nu = \frac{1}{4}$ (recall Remark 2.2) is $W^{C\varepsilon} = 8E\bar{s}^2/5$, where E is the Young's modulus. Assuming $W = W^{C\varepsilon}$, we find that

$$(2.9) \quad c = \frac{16E}{5\pi h \int_0^\delta \omega(r) r^2 dr} \quad \text{for a 2D problem in a state of plane strain.}$$

Plane stress. For a body in a state of plane stress and under an isotropic extension given by $\mathbf{u}(\mathbf{x}) = \bar{s}\mathbf{x}$ for some $\bar{s} > 0$, it is known from classical linear elasticity that the strain energy density for materials with a Poisson's ratio of $\nu = \frac{1}{3}$ (recall Remark 2.2) is $W^{C\sigma} = 3E\bar{s}^2/2$. Assuming $W = W^{C\sigma}$, we find that

$$(2.10) \quad c = \frac{3E}{\pi h \int_0^\delta \omega(r) r^2 dr} \quad \text{for a 2D problem in a state of plane stress.}$$

Remark 2.3. As noted in [36], although the expressions for the micromodulus constant c in (2.9) and (2.10) depend on h , in practice, h does not appear in (2.2) and (2.5) because, after substituting the expression of the GPMC pairwise force function (see (2.6)) and micropotential (see (2.7)) into these equations, respectively, the product hc emerges, which is h -independent.

3. BOND-FAILURE CRITERIA FOR THREE-DIMENSIONAL PROBLEMS

In this section, we analyze the two bond-failure criteria—critical stretch and critical energy density—in three dimensions. For consistency, for both criteria, we assume that bonds break once they reach a critical threshold.

3.1. Bond-failure criteria. The bond-failure criteria are distinguished by their choice of Boolean-valued function μ in (2.6) and (2.7). In the critical stretch criterion [39], there is a constant $s_0 > 0$ (the critical stretch) such that μ is given by

$$(3.1) \quad \mu(\mathbf{x}', \mathbf{x}, t) = \mu_0(\mathbf{x}', \mathbf{x}, t) := \begin{cases} 1 & \text{if } s(\tilde{\boldsymbol{\eta}}, \boldsymbol{\xi}) < s_0 \text{ for all } 0 \leq \tilde{t} \leq t, \\ 0 & \text{otherwise,} \end{cases}$$

where $\tilde{\boldsymbol{\eta}} := \mathbf{u}(\mathbf{x}', \tilde{t}) - \mathbf{u}(\mathbf{x}, \tilde{t})$. On the other hand, in the critical energy density criterion [8], there is a constant $w_c > 0$ (the critical energy density) such that μ is given by

$$(3.2) \quad \mu(\mathbf{x}', \mathbf{x}, t) = \mu_c(\mathbf{x}', \mathbf{x}, t) := \begin{cases} 1 & \text{if } w(\tilde{\boldsymbol{\eta}}, \mathbf{x}', \mathbf{x}, \tilde{t}) < w_c \text{ for all } 0 \leq \tilde{t} \leq t, \\ 0 & \text{otherwise.} \end{cases}$$

In both cases, we determine the critical values s_0 and w_c in terms of material constants. Towards this end, we first describe the work required to break all bonds across a fracture surface.

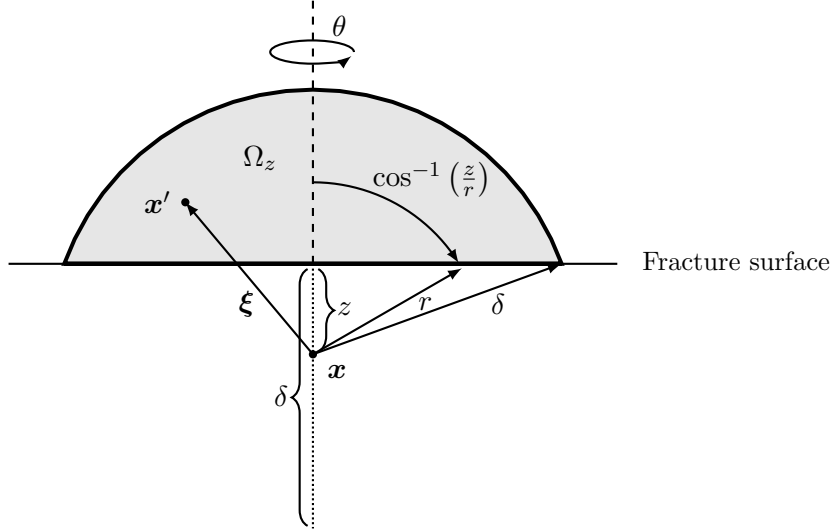


FIGURE 1. Description of all bonds ξ connecting a point \mathbf{x} located at a distance $z \in (0, \delta)$ below the fracture surface to points \mathbf{x}' in the spherical cap Ω_z above the fracture surface.

Split the body into two halves across a flat fracture surface (see Figure 1). To physically separate the halves, we require that all bonds across the fracture surface break (i.e., reach

the critical stretch s_0 or the critical energy density w_c). Consider a line segment of length δ below the fracture surface that is perpendicular to the fracture surface. Fix $z \in (0, \delta)$. Let $\mathbf{x} = \mathbf{x}(z)$ denote the unique point on the line at a distance z from the fracture surface, and let Ω_z denote the spherical cap of radius δ centered at \mathbf{x} above the fracture surface (see Figure 1). For fracture to occur, all bonds connecting $\mathbf{x} = \mathbf{x}(z)$ to points \mathbf{x}' in Ω_z must break for every $z \in (0, \delta)$. The corresponding energy per unit fracture area required to break all those bonds, or the energy release rate, is given by

$$(3.3) \quad G_0 = \int_0^\delta \int_{\Omega_z} w_{\text{critical}}(\mathbf{x}', \mathbf{x}(z)) dV_{\mathbf{x}'} dz,$$

where $w_{\text{critical}} = w_{\text{critical}}(\mathbf{x}', \mathbf{x})$ is the energy density stored in the bond $\xi = \mathbf{x}' - \mathbf{x}$ when it reaches the critical stretch or the critical energy density according to μ in (3.1) or (3.2), respectively.

3.1.1. *Critical stretch criterion.* Consider first the critical stretch criterion. If a bond is at the critical stretch s_0 , then from (2.7), the energy density w_{critical} stored in the bond (assuming the bond has not broken) is

$$(3.4) \quad w_{\text{critical}}(\mathbf{x}', \mathbf{x}) = w_0(\|\xi\|) := \frac{1}{2} c \omega(\|\xi\|) s_0^2 \|\xi\|.$$

Using (3.3) together with (3.4), we conduct a standard computation using spherical coordinates to find (see [39]):

$$G_0 = \int_0^\delta \int_0^{2\pi} \int_z^\delta \int_0^{\cos^{-1}(z/r)} w_0(r) r^2 \sin(\phi) d\phi dr d\theta dz = \frac{\pi c s_0^2}{2} \int_0^\delta \omega(r) r^4 dr.$$

Recalling (2.8), we conclude that s_0 can be written in terms of material constants as

$$(3.5) \quad s_0^2 = \frac{4G_0}{9K} \frac{\int_0^\delta \omega(r) r^3 dr}{\int_0^\delta \omega(r) r^4 dr} \quad \text{for a 3D problem.}$$

For $\omega(r) \equiv 1$, this recovers the expression in [39, Equation (27)].

3.1.2. *Critical energy density criterion.* Next, consider the critical energy density criterion. In this case, $w_{\text{critical}} \equiv w_c$ is constant. Using w_c in (3.3), we apply a standard computation using spherical coordinates to find (see [8]):

$$G_0 = \int_0^\delta \int_0^{2\pi} \int_z^\delta \int_0^{\cos^{-1}(z/r)} w_c r^2 \sin(\phi) d\phi dr d\theta dz = \frac{\pi w_c \delta^4}{4}.$$

Therefore, w_c can be written in terms of material constants as

$$(3.6) \quad w_c = \frac{4G_0}{\pi \delta^4} \quad \text{for a 3D problem.}$$

In the next lemma, we write the critical energy density criterion equivalently as a bond-dependent critical stretch criterion in which the critical stretch depends only on the bond length.

Lemma 3.1 (3D critical energy density criterion as a critical stretch criterion). *Given the pairwise force function (2.6), a bond $\xi = \mathbf{x}' - \mathbf{x} \in \mathcal{H} \setminus \{\mathbf{0}\}$, and a time $t > 0$, it holds that*

$$(3.7) \quad w(\boldsymbol{\eta}, \mathbf{x}', \mathbf{x}, t) < w_c \quad \text{if and only if} \quad s^2(\boldsymbol{\eta}, \xi) < s_c^2(\|\xi\|),$$

where

$$(3.8) \quad s_c^2(\|\boldsymbol{\xi}\|) = \frac{16G_0}{9K\delta^4\omega(\|\boldsymbol{\xi}\|)\|\boldsymbol{\xi}\|} \int_0^\delta \omega(r)r^3 dr.$$

Consequently, μ_c in (3.2) can be written as

$$(3.9) \quad \mu_c(\mathbf{x}', \mathbf{x}, t) = \begin{cases} 1 & \text{if } s^2(\tilde{\boldsymbol{\eta}}, \boldsymbol{\xi}) < s_c^2(\|\boldsymbol{\xi}\|) \text{ for all } 0 \leq \tilde{t} \leq t, \\ 0 & \text{otherwise.} \end{cases}$$

Proof. Fix a bond $\boldsymbol{\xi} \in \mathcal{H} \setminus \{\mathbf{0}\}$ and a time $t > 0$, and recall that $\omega(\|\boldsymbol{\xi}\|) > 0$. Consider the condition

$$(3.10) \quad w(\boldsymbol{\eta}, \mathbf{x}', \mathbf{x}, t) < w_c.$$

Recalling (2.7), (2.8), (3.6), and that $\mu = 1$ for an intact bond, we have that the inequality (3.10) holds if and only if

$$\frac{1}{2} \frac{9K}{2\pi \int_0^\delta \omega(r)r^3 dr} \omega(\|\boldsymbol{\xi}\|) s^2(\boldsymbol{\eta}, \boldsymbol{\xi}) \|\boldsymbol{\xi}\| < \frac{4G_0}{\pi\delta^4}.$$

Equivalently,

$$s^2(\boldsymbol{\eta}, \boldsymbol{\xi}) < \frac{16G_0}{9K\delta^4\omega(\|\boldsymbol{\xi}\|)\|\boldsymbol{\xi}\|} \int_0^\delta \omega(r)r^3 dr = s_c^2(\|\boldsymbol{\xi}\|).$$

□

Remark 3.2. From (3.8) and (3.5), the quantities s_c and s_0 are related in the following way:

$$(3.11) \quad s_c^2(\|\boldsymbol{\xi}\|) = \frac{4}{\delta^4\omega(\|\boldsymbol{\xi}\|)\|\boldsymbol{\xi}\|} \left(\frac{4G_0}{9K} \int_0^\delta \omega(r)r^3 dr \right) = \left(\frac{4}{\delta^4\omega(\|\boldsymbol{\xi}\|)\|\boldsymbol{\xi}\|} \int_0^\delta \omega(r)r^4 dr \right) s_0^2.$$

3.2. Critical stretch vs. critical energy density criteria. We now present our main result.

Theorem 3.3 (Nonequivalence of bond-failure criteria for 3D problems). *Given the pairwise force function (2.6), the bond-breaking functions μ_0 and μ_c coincide if and only if there exists a constant $\beta > 0$ such that $\omega(\|\boldsymbol{\xi}\|) = \beta\|\boldsymbol{\xi}\|^{-1}$ for all $\boldsymbol{\xi} \in \mathcal{H} \setminus \{\mathbf{0}\}$. In this case, the bond-breaking function μ can be written as*

$$\mu(\mathbf{x}', \mathbf{x}, t) = \mu_0(\mathbf{x}', \mathbf{x}, t) = \mu_c(\mathbf{x}', \mathbf{x}, t) = \begin{cases} 1 & \text{if } s^2(\tilde{\boldsymbol{\eta}}, \boldsymbol{\xi}) < s_0^2 \text{ for all } 0 \leq \tilde{t} \leq t, \\ 0 & \text{otherwise,} \end{cases}$$

where

$$s_0^2 = s_c^2(\|\boldsymbol{\xi}\|) = \frac{16G_0}{27K\delta}.$$

Proof. By Lemma 3.1, the critical stretch and critical energy density criteria coincide if and only if $s_0^2 = s_c^2(\|\boldsymbol{\xi}\|)$ for all $\boldsymbol{\xi} \in \mathcal{H} \setminus \{\mathbf{0}\}$. Thus, we will prove

$$s_0^2 = s_c^2(\|\boldsymbol{\xi}\|) \text{ for all } \boldsymbol{\xi} \in \mathcal{H} \setminus \{\mathbf{0}\} \quad \text{if and only if} \quad \omega(\|\boldsymbol{\xi}\|) = \beta\|\boldsymbol{\xi}\|^{-1} \text{ for all } \boldsymbol{\xi} \in \mathcal{H} \setminus \{\mathbf{0}\}$$

for some constant $\beta > 0$. Assume first that there exists some constant $\beta > 0$ such that $\omega(\|\boldsymbol{\xi}\|) = \beta\|\boldsymbol{\xi}\|^{-1}$ for all $\boldsymbol{\xi} \in \mathcal{H} \setminus \{\mathbf{0}\}$. From (3.11), we have

$$s_c^2(\|\boldsymbol{\xi}\|) = \frac{4s_0^2}{\delta^4\beta} \int_0^\delta \beta r^3 dr = s_0^2 \quad \text{for all } \boldsymbol{\xi} \in \mathcal{H} \setminus \{\mathbf{0}\},$$

as desired. Conversely, assume that $s_0^2 = s_c^2(\|\boldsymbol{\xi}\|)$ for all $\boldsymbol{\xi} \in \mathcal{H} \setminus \{\mathbf{0}\}$. By (3.11), we have

$$1 = \frac{4}{\delta^4 \omega(\|\boldsymbol{\xi}\|) \|\boldsymbol{\xi}\|} \int_0^\delta \omega(r) r^4 dr \quad \text{for all } \boldsymbol{\xi} \in \mathcal{H} \setminus \{\mathbf{0}\}.$$

Rearranging, we write

$$\omega(\|\boldsymbol{\xi}\|) \|\boldsymbol{\xi}\| = \frac{4}{\delta^4} \int_0^\delta \omega(r) r^4 dr \quad \text{for all } \boldsymbol{\xi} \in \mathcal{H} \setminus \{\mathbf{0}\}$$

to find that $\omega(\|\boldsymbol{\xi}\|) \|\boldsymbol{\xi}\|$ is constant in $\mathcal{H} \setminus \{\mathbf{0}\}$, i.e., there exists some constant $\beta > 0$ such that $\omega(\|\boldsymbol{\xi}\|) = \beta \|\boldsymbol{\xi}\|^{-1}$ for all $\boldsymbol{\xi} \in \mathcal{H} \setminus \{\mathbf{0}\}$.

Lastly, note that if $\omega(\|\boldsymbol{\xi}\|) \|\boldsymbol{\xi}\| = \beta$, then from (3.5), we have

$$s_c^2(\|\boldsymbol{\xi}\|) = s_0^2 = \frac{4G_0}{9K} \frac{\int_0^\delta \beta r^2 dr}{\int_0^\delta \beta r^3 dr} = \frac{16G_0}{27K\delta}.$$

□

Theorem 3.3 establishes that the critical stretch and critical energy density criteria are *not* equivalent in general. For example, consider the influence function

$$(3.12) \quad \omega(\|\boldsymbol{\xi}\|) = \|\boldsymbol{\xi}\|^{-\alpha} \quad \text{for some } \alpha \in (-\infty, 1) \cup (1, 4).$$

By Theorem 3.3, if $\alpha = 1$, then the two criteria are equivalent, so we omit that case. On the other hand, by (2.8), it must be that $\alpha < 4$. In this setting, one has, by (3.5),

$$(3.13) \quad s_0^2 = \frac{4G_0}{9K} \frac{\int_0^\delta r^{3-\alpha} dr}{\int_0^\delta r^{4-\alpha} dr} = \frac{4G_0(5-\alpha)}{9K(4-\alpha)\delta},$$

and by (3.11),

$$(3.14) \quad s_c^2(\|\boldsymbol{\xi}\|) = \left(\frac{4}{\delta^4 \|\boldsymbol{\xi}\|^{1-\alpha}} \int_0^\delta r^{4-\alpha} dr \right) s_0^2 = \frac{4}{5-\alpha} \left(\frac{\delta}{\|\boldsymbol{\xi}\|} \right)^{1-\alpha} s_0^2,$$

demonstrating that s_c^2 and s_0^2 do not coincide, except for $\alpha = 1$.

Moreover,

$$(3.15) \quad s_c^2(\|\boldsymbol{\xi}\|) > s_0^2 \quad \text{if and only if} \quad \frac{4\delta^{1-\alpha}}{5-\alpha} > \|\boldsymbol{\xi}\|^{1-\alpha}.$$

Therefore, if $\alpha < 1$, then, from (3.15), we see that “sufficiently short” bonds break first under the critical stretch criterion and “sufficiently long” bonds break first under the critical energy density criterion. On the other hand, if $1 < \alpha < 4$, then we see from (3.15) that “sufficiently long” bonds break first under the critical stretch criterion and “sufficiently short” bonds break first under the critical energy density criterion. With these ingredients, we make precise Theorem 1.2 for 3D problems:

Theorem 3.4 (Bond-breaking behavior for 3D problems). *Consider the pairwise force function (2.6) with influence function (3.12).*

(1) Assume that $\alpha < 1$. A bond $\xi = \mathbf{x}' - \mathbf{x}$ satisfying

$$\|\xi\| < \left(\frac{4}{5-\alpha} \right)^{\frac{1}{1-\alpha}} \delta$$

and $s^2(\eta, \xi) = s_0^2$ at time $t > 0$ breaks at time t under the critical stretch criterion but does not break under the critical energy density criterion. On the other hand, a bond satisfying

$$\left(\frac{4}{5-\alpha} \right)^{\frac{1}{1-\alpha}} \delta < \|\xi\| \leq \delta$$

and $s^2(\eta, \xi) = s_c^2(\|\xi\|)$ at time $t > 0$ breaks at time t under the critical energy density criterion but does not break under the critical stretch criterion.

(2) Assume that $1 < \alpha < 4$. A bond $\xi = \mathbf{x}' - \mathbf{x}$ satisfying

$$\left(\frac{5-\alpha}{4} \right)^{\frac{1}{\alpha-1}} \delta < \|\xi\| \leq \delta$$

and $s^2(\eta, \xi) = s_0^2$ at time $t > 0$ breaks at time t under the critical stretch criterion but does not break under the critical energy density criterion. On the other hand, a bond satisfying

$$\|\xi\| < \left(\frac{5-\alpha}{4} \right)^{\frac{1}{\alpha-1}} \delta$$

and $s^2(\eta, \xi) = s_c^2(\|\xi\|)$ at time $t > 0$ breaks at time t under the critical energy density criterion but does not break under the critical stretch criterion.

3.2.1. *Isotropic extension.* Consider still the influence function (3.12), and now let us assume an isotropic extension. Recalling Remark 2.1, $s \equiv \bar{s}$ for some constant $\bar{s} > 0$. Under the critical stretch criterion, all bonds $\xi \in \mathcal{H} \setminus \{\mathbf{0}\}$ break as long as $\bar{s} \geq s_0$. On the other hand, under the critical energy density criterion, a bond ξ breaks when $\bar{s}^2 \geq s_c^2(\|\xi\|) = 4s_0^2\delta^{1-\alpha}/((5-\alpha)\|\xi\|^{1-\alpha})$ (see (3.14)) or, equivalently,

$$(3.16) \quad \|\xi\|^{1-\alpha} \geq \frac{4\delta^{1-\alpha}s_0^2}{(5-\alpha)\bar{s}^2}.$$

Note that for the longest bonds (i.e., bonds $\xi \in \mathcal{H} \setminus \{\mathbf{0}\}$ such that $\|\xi\| = \delta$) to break, \bar{s} must satisfy (see (3.13))

$$(3.17) \quad \bar{s}^2 \geq \frac{4s_0^2}{5-\alpha} = \frac{16G_0}{9K(4-\alpha)\delta}.$$

Therefore, we conclude the following:

(1) Assume $\alpha < 1$. As long as (3.17) is satisfied, we use (3.16) to conclude that all bonds $\xi \in \mathcal{H} \setminus \{\mathbf{0}\}$ in the spherical shell

$$\left\{ \xi : \left(\frac{4s_0^2}{(5-\alpha)\bar{s}^2} \right)^{\frac{1}{1-\alpha}} \delta \leq \|\xi\| \leq \delta \right\}$$

break under the critical energy density criterion. That is, only sufficiently long bonds break.

(2) Assume $1 < \alpha < 4$. We use (3.16) to conclude that all bonds $\xi \in \mathcal{H} \setminus \{\mathbf{0}\}$ in the closed ball

$$\left\{ \xi : \|\xi\| \leq \left(\frac{(5-\alpha)\bar{s}^2}{4s_0^2} \right)^{\frac{1}{\alpha-1}} \delta \right\}$$

break under the critical energy density criterion. That is, only sufficiently short bonds break. Moreover, for all bonds $\xi \in \mathcal{H} \setminus \{\mathbf{0}\}$ to break, \bar{s} must satisfy (3.17).

4. BOND-FAILURE CRITERIA FOR TWO-DIMENSIONAL PROBLEMS

In this section, we analyze the bond-failure criteria as in Section 3, but for two-dimensional problems.

4.1. Bond-failure criteria. As in Section 3.1, we will use the energy release rate to determine the critical parameters s_0 and w_c in (3.1) and (3.2), respectively, in terms of material constants, but now for two-dimensional problems in a state of plane strain or plane stress. In analogy to (3.3), the energy per unit fracture area for a two-dimensional problem can be computed as

$$(4.1) \quad G_0 = h \int_0^\delta \int_{\Omega_z} w_{\text{critical}}(\mathbf{x}', \mathbf{x}(z)) dA_{\mathbf{x}'} dz,$$

where Ω_z now represents a circular segment (see Figure 1).

4.1.1. Critical stretch criterion. Assume first the critical stretch criterion, namely (3.1). Using (4.1) together with (3.4), we conduct a standard computation using polar coordinates (see [36, Appendix C.2]) to get:

$$G_0 = h \int_0^\delta \int_z^\delta \int_{-\cos^{-1}(z/r)}^{\cos^{-1}(z/r)} w_0(r) r d\theta dr dz = h c s_0^2 \int_0^\delta \omega(r) r^3 dr.$$

Recalling (2.9) and (2.10), we find

$$(4.2) \quad s_0^2 = \frac{G_0}{h c \int_0^\delta \omega(r) r^3 dr} = \begin{cases} \frac{5\pi G_0}{16E} \frac{\int_0^\delta \omega(r) r^2 dr}{\int_0^\delta \omega(r) r^3 dr} & \text{for a 2D problem in a state of plane strain,} \\ \frac{\pi G_0}{3E} \frac{\int_0^\delta \omega(r) r^2 dr}{\int_0^\delta \omega(r) r^3 dr} & \text{for a 2D problem in a state of plane stress.} \end{cases}$$

4.1.2. Critical energy density criterion. Assume now the critical energy density criterion, namely (3.2). Using $w_{\text{critical}} \equiv w_c$ in (4.1), we apply a standard computation using polar coordinates to find:

$$G_0 = h \int_0^\delta \int_z^\delta \int_{-\cos^{-1}(z/r)}^{\cos^{-1}(z/r)} w_c r d\theta dr dz = \frac{2h w_c \delta^3}{3}.$$

Therefore, we have

$$(4.3) \quad w_c = \frac{3G_0}{2h\delta^3} \quad \text{for a 2D problem.}$$

Note that the critical energy density is the same for plane strain and plane stress.

Remark 4.1. The critical energy density in (4.3) depends on h , in contrast to the critical stretch, which does not depend on h (see (4.2)). Nevertheless, recasting the critical energy density criterion as a critical stretch criterion removes the dependence on h (see Lemma 4.2).

The following result, analogous to Lemma 3.1 for two-dimensional problems, holds.

Lemma 4.2 (2D critical energy density criterion as a critical stretch criterion). *Consider a two-dimensional problem involving a body in a state of plane strain or plane stress. Given the pairwise force function (2.6), a bond $\xi = \mathbf{x}' - \mathbf{x} \in \mathcal{H} \setminus \{\mathbf{0}\}$, and a time $t > 0$, it holds that*

$$w(\boldsymbol{\eta}, \mathbf{x}', \mathbf{x}, t) < w_c \quad \text{if and only if} \quad s^2(\boldsymbol{\eta}, \xi) < s_c^2(\|\xi\|),$$

where

$$(4.4) \quad s_c^2(\|\xi\|) = \begin{cases} \frac{15\pi G_0}{16E\delta^3\omega(\|\xi\|)\|\xi\|} \int_0^\delta \omega(r)r^2 dr & \text{for a 2D problem in a state of plane strain,} \\ \frac{\pi G_0}{E\delta^3\omega(\|\xi\|)\|\xi\|} \int_0^\delta \omega(r)r^2 dr & \text{for a 2D problem in a state of plane stress.} \end{cases}$$

Proof. Recalling the proof of Lemma 3.1, it is enough to note that, for a fixed bond $\xi \in \mathcal{H} \setminus \{\mathbf{0}\}$ and a fixed time $t > 0$, by (2.7) and (4.3) (recall that $\mu = 1$ for an intact bond and $\omega(\|\xi\|) > 0$),

$$w(\boldsymbol{\eta}, \mathbf{x}', \mathbf{x}, t) < w_c$$

holds if and only if

$$\frac{1}{2}c\omega(\|\xi\|)s^2(\boldsymbol{\eta}, \xi)\|\xi\| < \frac{3G_0}{2h\delta^3},$$

where c is given in (2.9) for plane strain and (2.10) for plane stress. Equivalently,

$$(4.5) \quad s^2(\boldsymbol{\eta}, \xi) < \frac{3G_0}{hc\delta^3\omega(\|\xi\|)\|\xi\|} = s_c^2(\|\xi\|).$$

The expression (4.4) follows from (4.5) together with (2.9) and (2.10). □

Remark 4.3. Note from (4.5) and (4.2) that

$$(4.6) \quad s_c^2(\|\xi\|) = \frac{3}{\delta^3\omega(\|\xi\|)\|\xi\|} \frac{G_0}{hc} = \left(\frac{3}{\delta^3\omega(\|\xi\|)\|\xi\|} \int_0^\delta \omega(r)r^3 dr \right) s_0^2.$$

Comparing (3.11) and (4.6), we conclude:

$$s_c^2(\|\xi\|) = \left(\frac{d+1}{\delta^{d+1}\omega(\|\xi\|)\|\xi\|} \int_0^\delta \omega(r)r^{d+1} dr \right) s_0^2, \quad \text{for } d = 2, 3.$$

4.2. Critical stretch vs. critical energy density criteria. We have the following two-dimensional analogue of Theorem 3.3.

Theorem 4.4 (Nonequivalence of bond-failure criteria for 2D problems). *Consider a two-dimensional problem involving a body in a state of plane strain or plane stress. Given the pairwise force function (2.6), the bond-breaking functions μ_0 and μ_c coincide if and only if there exists a constant $\beta > 0$ such that $\omega(\|\xi\|) = \beta\|\xi\|^{-1}$ for all $\xi \in \mathcal{H} \setminus \{\mathbf{0}\}$. In this case, the bond-breaking function μ can be written as*

$$\mu(\mathbf{x}', \mathbf{x}, t) = \mu_0(\mathbf{x}', \mathbf{x}, t) = \mu_c(\mathbf{x}', \mathbf{x}, t) = \begin{cases} 1 & \text{if } s^2(\tilde{\boldsymbol{\eta}}, \xi) < s_0^2 \text{ for all } 0 \leq \tilde{t} \leq t, \\ 0 & \text{otherwise,} \end{cases}$$

where

$$s_0^2 = s_c^2(\|\boldsymbol{\xi}\|) = \begin{cases} \frac{15\pi G_0}{32E\delta} & \text{for a 2D problem in a state of plane strain,} \\ \frac{\pi G_0}{2E\delta} & \text{for a 2D problem in a state of plane stress.} \end{cases}$$

Proof. By Lemma 4.2, the critical stretch and critical energy density criteria coincide if and only if $s_0^2 = s_c^2(\|\boldsymbol{\xi}\|)$ for all $\boldsymbol{\xi} \in \mathcal{H} \setminus \{\mathbf{0}\}$. Recalling the proof of Theorem 3.3, it is enough to observe that, if there is a $\beta > 0$ such that $\omega(\|\boldsymbol{\xi}\|) = \beta\|\boldsymbol{\xi}\|^{-1}$ for all $\boldsymbol{\xi} \in \mathcal{H} \setminus \{\mathbf{0}\}$, then from (4.6)

$$s_c^2(\|\boldsymbol{\xi}\|) = \left(\frac{3}{\delta^3\beta} \int_0^\delta \beta r^2 dr \right) s_0^2 = s_0^2$$

and from (4.2)

$$s_0^2 = \begin{cases} \frac{5\pi G_0}{16E} \frac{\int_0^\delta \beta r dr}{\int_0^\delta \beta r^2 dr} & \text{for plane strain,} \\ \frac{\pi G_0}{3E} \frac{\int_0^\delta \beta r dr}{\int_0^\delta \beta r^2 dr} & \text{for plane stress} \end{cases} = \begin{cases} \frac{15\pi G_0}{32E\delta} & \text{for plane strain,} \\ \frac{\pi G_0}{2E\delta} & \text{for plane stress.} \end{cases}$$

□

As observed in the previous section, Theorem 4.4 implies that the critical stretch and critical energy density criteria are *not* equivalent in general. Similar to Section 3.2, consider the influence function

$$(4.7) \quad \omega(\|\boldsymbol{\xi}\|) = \|\boldsymbol{\xi}\|^{-\alpha} \quad \text{for some } \alpha \in (-\infty, 1) \cup (1, 3).$$

By Theorem 4.4, if $\alpha = 1$, then the two criteria are equivalent, so we omit that case. On the other hand, by (2.9) and (2.10), it must be that $\alpha < 3$. In this setting, by (4.2), one can write

$$(4.8) \quad s_0^2 = \begin{cases} \frac{5\pi G_0(4-\alpha)}{16E(3-\alpha)\delta} & \text{for a 2D problem in a state of plane strain,} \\ \frac{\pi G_0(4-\alpha)}{3E(3-\alpha)\delta} & \text{for a 2D problem in a state of plane stress,} \end{cases}$$

and by (4.6),

$$(4.9) \quad s_c^2(\|\boldsymbol{\xi}\|) = \left(\frac{3}{\delta^3\|\boldsymbol{\xi}\|^{1-\alpha}} \int_0^\delta r^{3-\alpha} dr \right) s_0^2 = \frac{3}{4-\alpha} \left(\frac{\delta}{\|\boldsymbol{\xi}\|} \right)^{1-\alpha} s_0^2,$$

demonstrating that, also in the two-dimensional case, s_c^2 and s_0^2 do not coincide, except for $\alpha = 1$.

Moreover,

$$(4.10) \quad s_c^2(\|\boldsymbol{\xi}\|) > s_0^2 \quad \text{if and only if} \quad \frac{3\delta^{1-\alpha}}{4-\alpha} > \|\boldsymbol{\xi}\|^{1-\alpha}.$$

Recalling the discussion before Theorem 3.4 for 3D problems, we draw similar conclusions from (4.10) for 2D problems. In particular, we make precise Theorem 1.2 for 2D problems:

Theorem 4.5 (Bond-breaking behavior for 2D problems). *Consider the pairwise force function (2.6) with influence function (4.7) for a two-dimensional problem involving a body in a state of plane strain or plane stress.*

(1) *Assume that $\alpha < 1$. A bond $\xi \in \mathcal{H} \setminus \{\mathbf{0}\}$ satisfying*

$$\|\xi\| < \left(\frac{3}{4-\alpha} \right)^{\frac{1}{1-\alpha}} \delta$$

and $s^2(\eta, \xi) = s_0^2$ at time $t > 0$ breaks at time t under the critical stretch criterion but does not break under the critical energy density criterion. On the other hand, a bond $\xi \in \mathcal{H} \setminus \{\mathbf{0}\}$ satisfying

$$\left(\frac{3}{4-\alpha} \right)^{\frac{1}{1-\alpha}} \delta < \|\xi\| \leq \delta$$

and $s^2(\eta, \xi) = s_c^2(\|\xi\|)$ at time $t > 0$ breaks at time t under the critical energy density criterion but does not break under the critical stretch criterion.

(2) *Assume $1 < \alpha < 3$. A bond $\xi \in \mathcal{H} \setminus \{\mathbf{0}\}$ satisfying*

$$\left(\frac{4-\alpha}{3} \right)^{\frac{1}{\alpha-1}} \delta < \|\xi\| \leq \delta$$

and $s^2(\eta, \xi) = s_0^2$ at time $t > 0$ breaks at time t under the critical stretch criterion but does not break under the critical energy density criterion. On the other hand, a bond $\xi \in \mathcal{H} \setminus \{\mathbf{0}\}$ satisfying

$$\|\xi\| < \left(\frac{4-\alpha}{3} \right)^{\frac{1}{\alpha-1}} \delta$$

and $s^2(\eta, \xi) = s_c^2(\|\xi\|)$ at time $t > 0$ breaks at time t under the critical energy density criterion but does not break under the critical stretch criterion

4.2.1. *Isotropic extension.* Consider still the influence function (4.7), and now let us assume an isotropic extension. Recalling Remark 2.1, $s \equiv \bar{s}$ for some constant $\bar{s} > 0$. Under the critical stretch criterion, all bonds $\xi \in \mathcal{H} \setminus \{\mathbf{0}\}$ break as long as $\bar{s} \geq s_0$. On the other hand, under the critical energy density criterion, a bond ξ breaks when $\bar{s}^2 \geq s_c^2(\|\xi\|) = 3s_0^2\delta^{1-\alpha}/((4-\alpha)\|\xi\|^{1-\alpha})$ (see (4.9)) or, equivalently,

$$(4.11) \quad \|\xi\|^{1-\alpha} \geq \frac{3\delta^{1-\alpha}s_0^2}{(4-\alpha)\bar{s}^2}.$$

Note that for the longest bonds (i.e., bonds $\xi \in \mathcal{H} \setminus \{\mathbf{0}\}$ such that $\|\xi\| = \delta$) to break, \bar{s} must satisfy (see (4.8))

$$(4.12) \quad \bar{s}^2 \geq \frac{3s_0^2}{4-\alpha} = \begin{cases} \frac{15\pi G_0}{16E(3-\alpha)\delta} & \text{for a 2D problem in a state of plane strain,} \\ \frac{\pi G_0}{E(3-\alpha)\delta} & \text{for a 2D problem in a state of plane stress.} \end{cases}$$

Therefore, we conclude the following:

(1) Assume $\alpha < 1$. As long as (4.12) is satisfied, we use (4.11) to conclude that all bonds $\xi \in \mathcal{H} \setminus \{\mathbf{0}\}$ in the annulus

$$\left\{ \xi : \left(\frac{3s_0^2}{(4-\alpha)\bar{s}^2} \right)^{\frac{1}{1-\alpha}} \delta \leq \|\xi\| \leq \delta \right\}$$

break under the critical energy density criterion. That is, only sufficiently long bonds break.

(2) Assume $1 < \alpha < 3$. We use (4.11) to conclude that all bonds $\xi \in \mathcal{H} \setminus \{\mathbf{0}\}$ in the closed disc

$$\left\{ \xi : \|\xi\| \leq \left(\frac{(4-\alpha)\bar{s}^2}{3s_0^2} \right)^{\frac{1}{\alpha-1}} \delta \right\}$$

break under the critical energy density criterion. That is, only sufficiently short bonds break. Moreover, for all bonds $\xi \in \mathcal{H} \setminus \{\mathbf{0}\}$ to break, \bar{s} must satisfy (4.12).

This behavior will be observed numerically in Section 5.1.

5. NUMERICAL EXAMPLES

We now present three numerical examples in two dimensions. The material model for each example is the GPMB model given by (2.6) with the influence function $\omega(\|\xi\|) = 1/\|\xi\|^\alpha$, where $\alpha < 3$.

5.1. Example 1: Isotropic extension. In this example, we demonstrate the difference between the critical stretch and critical energy density criteria, including the effect of the choice of influence function on bond breaking, using a simple scenario with an imposed displacement field.

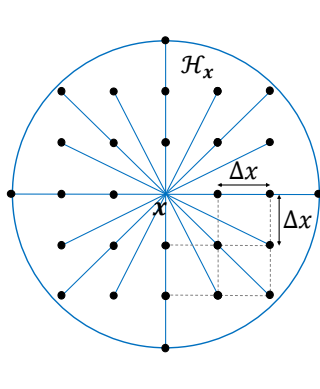
We consider a two-dimensional square plate with domain $\Omega = (-0.5, 0.5) \times (-0.5, 0.5)$ and a horizon of $\delta = 0.2$. The expressions for the elastic and bond-breaking parameters, derived in Section 2.2 (see (2.9) and (2.10)) and Section 4.2 (see (4.2), (4.3), and (4.9)), respectively, are summarized in Table 1.

c	s_0^2	w_c	$s_c^2(\ \xi\)$
$\frac{16(3-\alpha)E}{5\pi h\delta^{3-\alpha}}$ plane strain	$\frac{5(4-\alpha)\pi G_0}{16(3-\alpha)E\delta}$ plane strain		
$\frac{3(3-\alpha)E}{\pi h\delta^{3-\alpha}}$ plane stress	$\frac{(4-\alpha)\pi G_0}{3(3-\alpha)E\delta}$ plane stress	$\frac{3G_0}{2h\delta^3}$	$\frac{3}{4-\alpha} \left(\frac{\delta}{\ \xi\ } \right)^{1-\alpha} s_0^2$

TABLE 1. Elastic and bond-breaking parameters for $\omega(\|\xi\|) = 1/\|\xi\|^\alpha$ in 2D.

The plate is subjected to an isotropic extension given by $\mathbf{u}(\mathbf{x}) = \bar{s}\mathbf{x}$ with \bar{s} constant, resulting in a constant stretch $s \equiv \bar{s}$ for every bond ξ (see Remark 2.1). We assume a critical stretch $s_0 = 0.25$, which implies that bonds break under the critical stretch criterion when their extension reaches 25% of their original (undeformed) length. We compare numerically the plate response for varying imposed stretch \bar{s} and for different choices of the influence function parameter α using the critical energy density criterion. As proved in Theorem 4.4, the case $\alpha = 1$ coincides with the critical stretch criterion, i.e., $s_c(\|\xi\|) = s_0$.

The computations employ the PDMATLAB2D code [36], using the meshfree discretization from [39] with a uniform grid spacing of $\Delta x = \Delta y = \delta/3$, which results in a 15×15 grid of computational nodes and an m -ratio of $m := \delta/\Delta x = 3$. A relatively coarse discretization is employed in this example to enable clear visualization of results (including computational nodes and bonds). In this setting, each computational node in the bulk of the plate has 28 neighbors, as illustrated in Figure 2a.



(a) Illustration of the 2D neighborhood \mathcal{H}_x of a computational node at x .

$\ \xi\ $	$\alpha = 0$	$\alpha = 1$	$\alpha = 2$
Δx	$\frac{9}{4}s_0^2$	s_0^2	$\frac{1}{2}s_0^2$
$\sqrt{2}\Delta x$	$\frac{9}{4\sqrt{2}}s_0^2$	s_0^2	$\frac{\sqrt{2}}{2}s_0^2$
$2\Delta x$	$\frac{9}{8}s_0^2$	s_0^2	s_0^2
$\sqrt{5}\Delta x$	$\frac{9}{4\sqrt{5}}s_0^2$	s_0^2	$\frac{\sqrt{5}}{2}s_0^2$
$2\sqrt{2}\Delta x$	$\frac{9}{8\sqrt{2}}s_0^2$	s_0^2	$\sqrt{2}s_0^2$
$3\Delta x$	$\frac{3}{4}s_0^2$	s_0^2	$\frac{3}{2}s_0^2$

(b) Expressions for $s_c^2(\|\xi\|)$ as functions of s_0^2 for $\alpha = 0, 1, 2$ and for the different bond lengths.

FIGURE 2. Uniform discretization with a grid spacing of $\Delta x = \Delta y = \delta/3$ in Example 1.

We note from Figure 2a that, for the chosen discretization, a full neighborhood contains bonds with lengths $\|\xi\| = \Delta x, \sqrt{2}\Delta x, 2\Delta x, \sqrt{5}\Delta x, 2\sqrt{2}\Delta x$, or $3\Delta x$. In Figure 2b, we present the expressions for $s_c^2(\|\xi\|)$ for each of these bond lengths as functions of s_0^2 (cf. Table 1) for $\delta = 3\Delta x$ and different values of α . We observe that for $\alpha = 1$, s_c remains constant regardless of the bond length; for $\alpha = 0$, s_c decreases as the bond length increases; and for $\alpha = 2$, s_c increases as the bond length increases. This confirms our analytical results in Section 4.2.1. Indeed, for an isotropic extension with imposed stretch \bar{s} of increasing value, under the critical energy density criterion, longer bonds break first for $\alpha = 0$, whereas shorter bonds break first for $\alpha = 2$. In contrast, for $\alpha = 1$, all bonds break at the same critical stretch.

In Figure 3, we present numerical results demonstrating these different bond-breaking patterns. Specific values of imposed stretch \bar{s} were selected based on Figure 2b. All the computational nodes and bonds are plotted in cyan. For better visualization, we also select a given source node and draw its neighborhood, including its boundary (blue circle) and the intact bonds (blue lines) and corresponding neighboring nodes (black filled circles). Examining the results from the top row to the bottom row, the computations confirm that longer bonds break first for $\alpha = 0$ (left column), whereas shorter bonds break first for $\alpha = 2$ (right column), as proved.

5.2. Example 2: Crack tip evolution. In this example, we compare the effect of the bond-failure criteria on the evolution of a crack tip. Accordingly, we consider the problem of crack propagation in a pre-notched soda-lime glass thin plate subjected to traction loading [2]. The details of this problem, including the discretization parameters, are provided in the next section, where we study the full behavior of the system. Here, however, we focus on the evolution of the crack tip during the initial steps that lead to crack propagation. Our goal

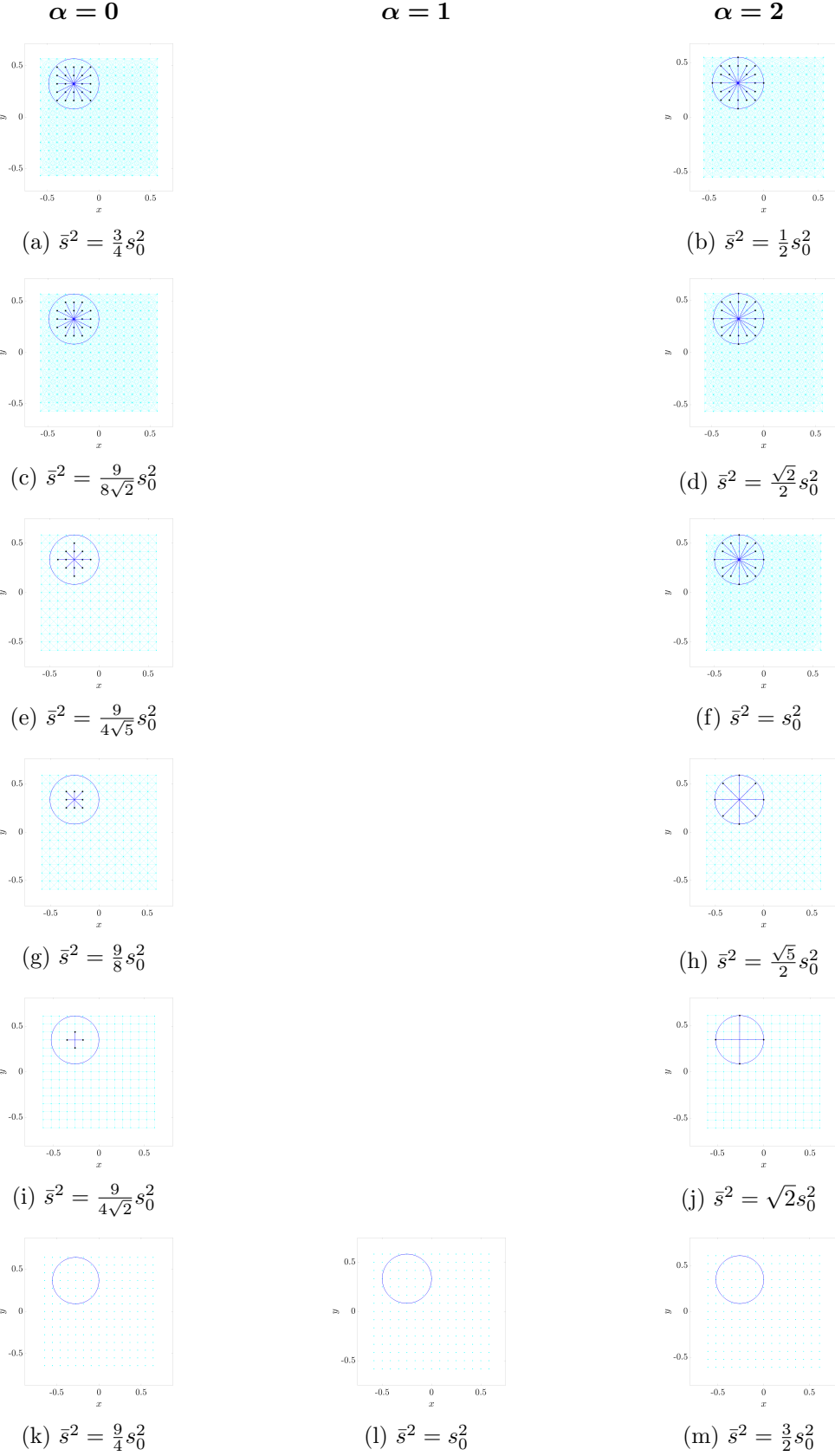


FIGURE 3. Illustration of the bond-breaking patterns for the critical energy density bond-failure criterion for different values of the influence function parameter α in Example 1.

is to illustrate the sequence of bond breaking for different choices of the influence function parameter α for the critical stretch and critical energy density criteria.

As opposed to the previous section, where the deformation is prescribed, here the deformation results from the material response to the imposed loading and, as such, depends on the material model chosen, in particular the influence function. Indeed, different choices of influence function can result in different elastic and fracture behavior [35]. It was observed experimentally for Homalite that crack propagation is affected by stress wave interactions (see, e.g., [30]); this phenomenon was confirmed numerically through peridynamic simulations in both soda-lime glass and Homalite (see, e.g., [2]). Therefore, in this section, rather than comparing simulation results for different influence functions, we study the difference between the bond-failure criteria for given choices of the influence function, i.e., for given values of α .

Here, we consider the case of a traction magnitude of $\sigma = 0.2$ MPa. The results are reported for $\alpha = 0$ in Figures 4 and 5, and for $\alpha = 2$ in Figures 6 and 7. For clarity, we specify the bonds that break at each step in Table 2 for $\alpha = 0$ and in Table 3 for $\alpha = 2$.

5.2.1. The case $\alpha = 0$. In the case of $\alpha = 0$, the bond energy density required for bond breaking is larger for the critical energy density criterion than for the critical stretch criterion (i.e., $s_c^2(\|\xi\|) > s_0^2$) for bonds of length $\sqrt{5}\Delta x$ or shorter (*cf.* Figure 2b). This is reflected in Figure 4, where although the first bonds to break (bonds of length $\sqrt{5}\Delta x$; see Table 2) are the same for both criteria, those bonds break earlier for the critical stretch criterion (step 928; see Figure 4a) than for the critical energy density criterion (step 930; see Figure 4b). A similar situation occurs during the next stage of bond breaking: although the same bond breaks next (bond of length Δx ; see Table 2), it breaks earlier for the critical stretch criterion (step 929; see Figure 4c) than for the critical energy density criterion (step 933; see Figure 4d). Note that the energy density required to break bonds of length $\sqrt{5}\Delta x$ or Δx for the critical energy density criterion is larger than that required to break either of these bonds for the critical stretch criterion (*cf.* Figure 2b). This is reflected in that no bonds break until step 930 for the critical energy density criterion, whereas bonds of length $\sqrt{5}\Delta x$ and Δx already break by step 929.

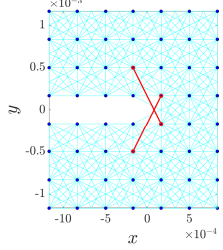
More precisely, Theorem 4.5 implies that, for $\alpha = 0$ and $\delta = 3\Delta x$, shorter bonds satisfying $\|\xi\| < 9\Delta x/4$ break earlier for the critical stretch criterion than for the critical energy density criterion, whereas the opposite holds for longer bonds satisfying $9\Delta x/4 < \|\xi\| \leq \delta$. This is consistent with the results observed in Figures 4 and 5. For instance, in Figure 5, we observe that, for the critical stretch criterion, shorter bonds (of length $\sqrt{2}\Delta x$; see Table 2) break at step 935 (see Figure 5a), followed by longer bonds (of length $2\sqrt{2}\Delta x$; see Table 2) that break at step 1036 (see Figure 5c); in contrast, the reversed scenario occurs for the critical energy density criterion (see Figures 5b and 5d).

A comparison of the strain energy density field at the time of initial bond breaking is provided in Figure 8. Since there is only a two time-step difference between the result for the critical stretch criterion (step 928) and the result for the critical energy density criterion (step 930), the two figures look alike.

5.2.2. The case $\alpha = 2$. In the case of $\alpha = 2$, the bond energy density required for bond breaking is smaller for the critical energy density criterion than for the critical stretch criterion (i.e., $s_c^2(\|\xi\|) < s_0^2$) for bonds of length Δx or $\sqrt{2}\Delta x$ (*cf.* Figure 2b). More precisely, Theorem 4.5 implies that, for $\alpha = 2$ and $\delta = 3\Delta x$, shorter bonds satisfying $\|\xi\| < 2\Delta x$ break earlier for the critical energy density criterion than for the critical stretch criterion, whereas the opposite holds for longer bonds satisfying $2\Delta x < \|\xi\| \leq \delta$. This is reflected in Figure 6, where the first bond to break for the critical energy density criterion (step 932; see Figure 6b)

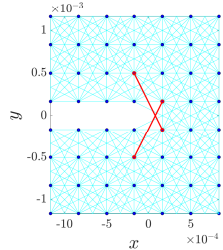
The case $\alpha = 0$

Critical stretch

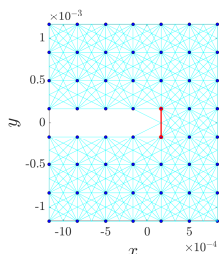


(a) step = 928

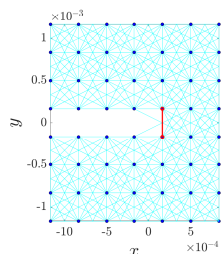
Critical energy density



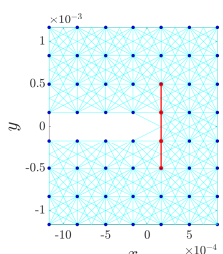
(b) step = 930



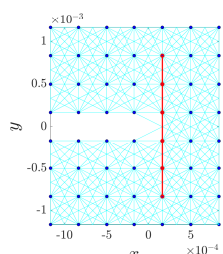
(c) step = 929



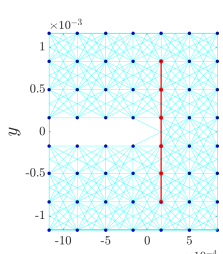
(d) step = 933



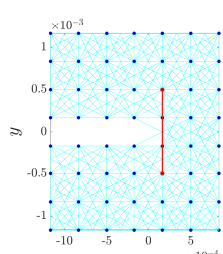
(e) step = 930



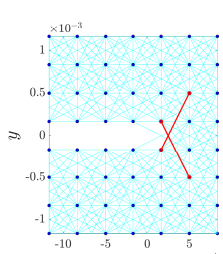
(f) step = 935



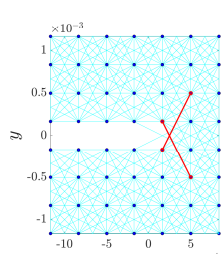
(g) step = 932



(h) step = 936



(i) step = 933



(j) step = 937

FIGURE 4. Comparison of the crack tip evolution between the two bond-failure criteria for $\alpha = 0$ in Example 2.

The case $\alpha = 0$ (cont.)

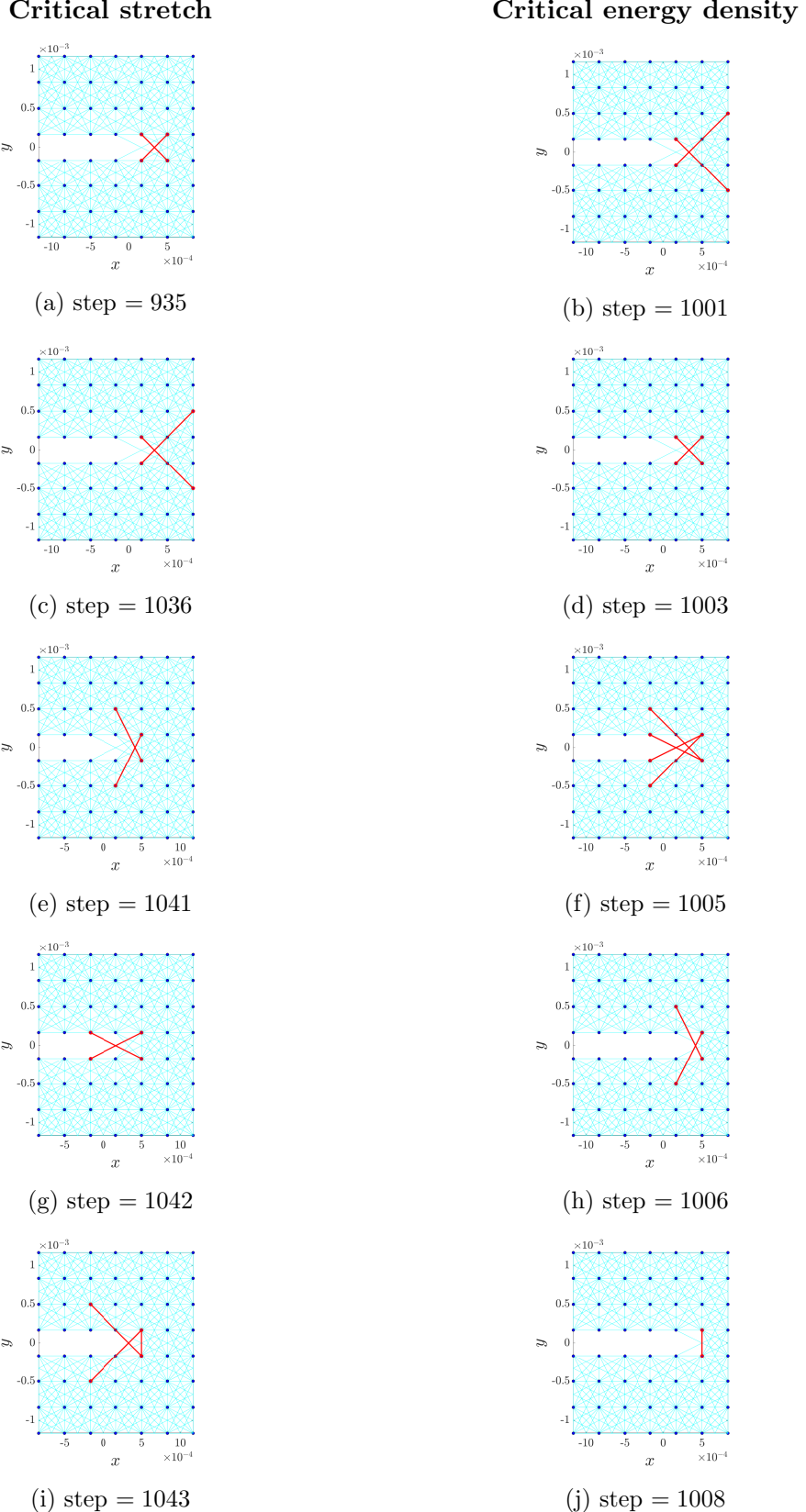


FIGURE 5. Comparison of the crack tip evolution between the two bond-failure criteria for $\alpha = 0$ in Example 2 (cont.).

	Step	Critical stretch criterion		Step	Critical energy density criterion	
		Bond	Bond length		Bond	Bond length
1	928	1: [17,550 ; 18,151]	$\sqrt{5}\Delta x$	930	1: [17,550 ; 18,151]	$\sqrt{5}\Delta x$
		2: [17,851 ; 18,450]	$\sqrt{5}\Delta x$		2: [17,851 ; 18,450]	$\sqrt{5}\Delta x$
2	929	1: [17,851 ; 18,151]	Δx	933	1: [17,851 ; 18,151]	Δx
3	930	1: [17,551 ; 18,151]	$2\Delta x$	935	1: [17,251 ; 18,151]	$3\Delta x$
		2: [17,851 ; 18,451]	$2\Delta x$		2: [17,551 ; 18,151]	$2\Delta x$
					3: [17,851 ; 18,451]	$2\Delta x$
					4: [17,851 ; 18,751]	$3\Delta x$
4	932	1: [17,251 ; 18,151]	$3\Delta x$	936	1: [17,551 ; 18,451]	$3\Delta x$
		2: [17,551 ; 18,451]	$3\Delta x$			
		3: [17,851 ; 18,751]	$3\Delta x$			
5	933	1: [17,552 ; 18,151]	$\sqrt{5}\Delta x$	937	1: [17,552 ; 18,151]	$\sqrt{5}\Delta x$
		2: [17,851 ; 18,452]	$\sqrt{5}\Delta x$		2: [17,851 ; 18,452]	$\sqrt{5}\Delta x$
6	935	1: [17,851 ; 18,152]	$\sqrt{2}\Delta x$	1001	1: [17,553 ; 18,151]	$2\sqrt{2}\Delta x$
		2: [17,852 ; 18,151]	$\sqrt{2}\Delta x$		2: [17,851 ; 18,453]	$2\sqrt{2}\Delta x$
7	1036	1: [17,553 ; 18,151]	$2\sqrt{2}\Delta x$	1003	1: [17,851 ; 18,152]	$\sqrt{2}\Delta x$
		2: [17,851 ; 18,453]	$2\sqrt{2}\Delta x$		2: [17,852 ; 18,151]	$\sqrt{2}\Delta x$
8	1041	1: [17,551 ; 18,152]	$\sqrt{5}\Delta x$	1005	1: [17,550 ; 18,152]	$2\sqrt{2}\Delta x$
		2: [17,852 ; 18,451]	$\sqrt{5}\Delta x$		2: [17,850 ; 18,152]	$\sqrt{5}\Delta x$
					3: [17,852 ; 18,150]	$\sqrt{5}\Delta x$
					4: [17,852 ; 18,450]	$2\sqrt{2}\Delta x$
9	1042	1: [17,850 ; 18,152]	$\sqrt{5}\Delta x$	1006	1: [17,551 ; 18,152]	$\sqrt{5}\Delta x$
		2: [17,852 ; 18,150]	$\sqrt{5}\Delta x$		2: [17,852 ; 18,451]	$\sqrt{5}\Delta x$
10	1043	1: [17,550 ; 18,152]	$2\sqrt{2}\Delta x$	1008	1: [17,852 ; 18,152]	Δx
		2: [17,852 ; 18,152]	Δx			
		3: [17,852 ; 18,450]	$2\sqrt{2}\Delta x$			

TABLE 2. List of broken bonds and corresponding bond lengths for the first 10 stages of bond breaking, for the case of $\alpha = 0$, for the two bond-failure criteria in Example 2 (*cf.* Figures 4 and 5). Bonds are listed with the numbers of the pair of computational nodes they connect.

The case $\alpha = 2$

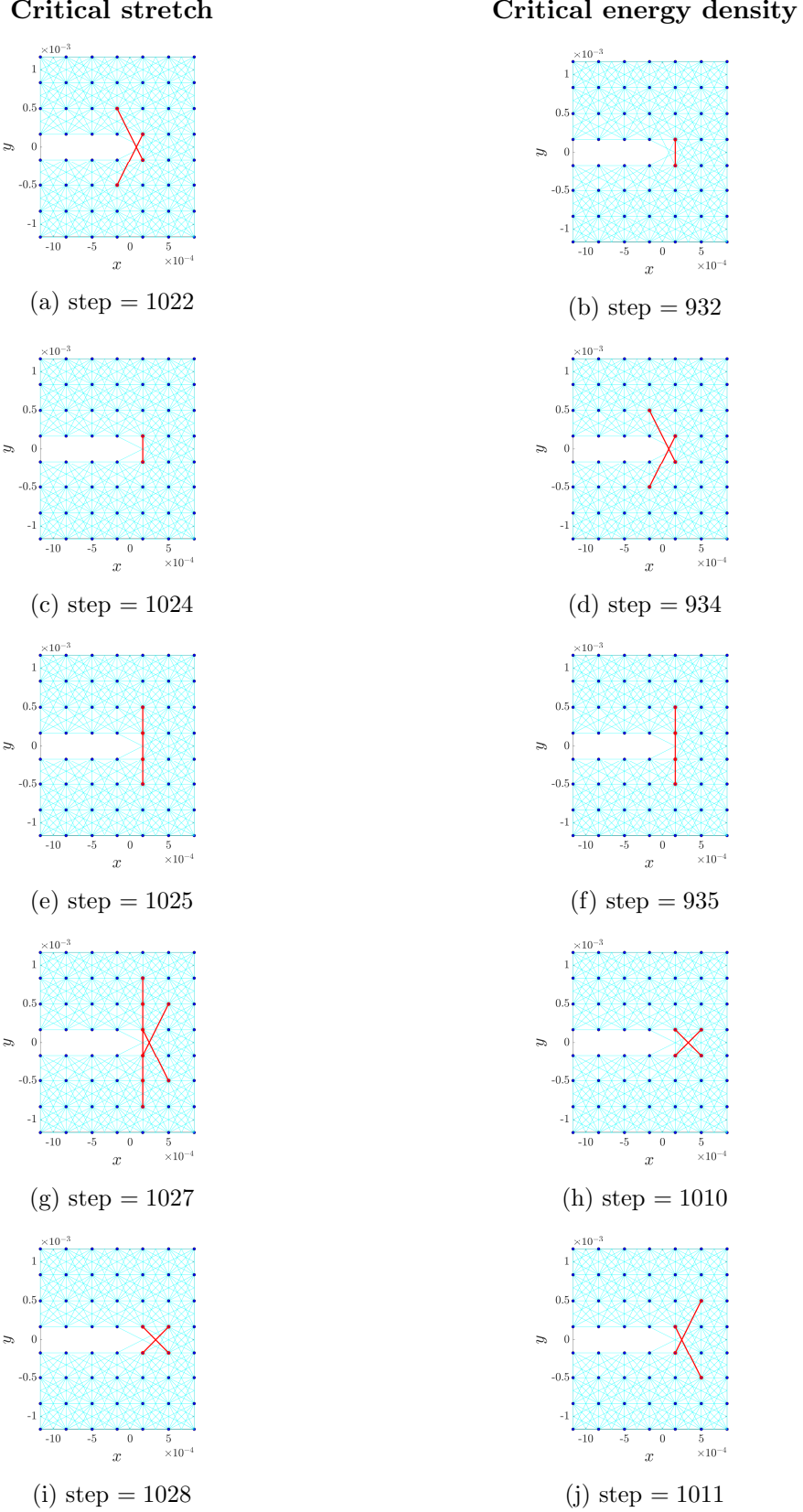
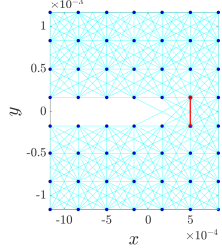


FIGURE 6. Comparison of the crack tip evolution between the two bond-failure criteria for $\alpha = 2$ in Example 2.

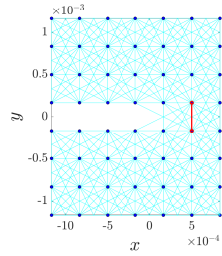
The case $\alpha = 2$ (cont.)

Critical stretch

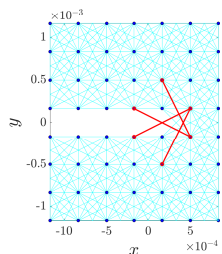


(a) step = 1030

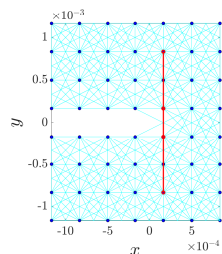
Critical energy density



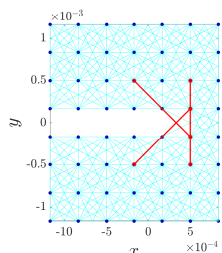
(b) step = 1012



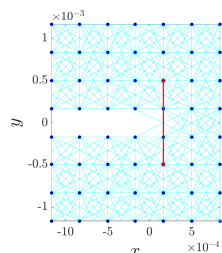
(c) step = 1031



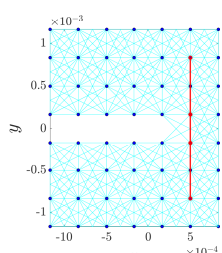
(d) step = 1013



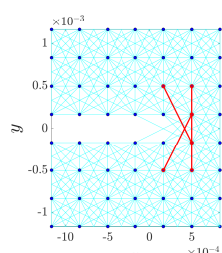
(e) step = 1032



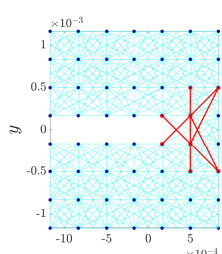
(f) step = 1014



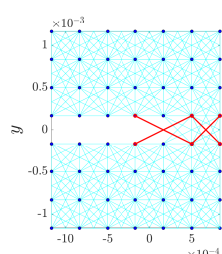
(g) step = 1033



(h) step = 1015



(i) step = 1034



(j) step = 1018

FIGURE 7. Comparison of the crack tip evolution between the two bond-failure criteria for $\alpha = 2$ in Example 2 (cont.).

	Step	Critical stretch criterion		Step	Critical energy density criterion	
		Bond	Bond length		Bond	Bond length
1	1022	1: [17,550 ; 18,151]	$\sqrt{5}\Delta x$	932	1: [17,851 ; 18,151]	Δx
		2: [17,851 ; 18,450]	$\sqrt{5}\Delta x$			
2	1024	1: [17,851 ; 18,151]	Δx	934	1: [17,550 ; 18,151]	$\sqrt{5}\Delta x$
					2: [17,851 ; 18,450]	$\sqrt{5}\Delta x$
3	1025	1: [17,551 ; 18,151]	$2\Delta x$	935	1: [17,551 ; 18,151]	$2\Delta x$
		2: [17,851 ; 18,451]	$2\Delta x$		2: [17,851 ; 18,451]	$2\Delta x$
4	1027	1: [17,251 ; 18,151]	$3\Delta x$	1010	1: [17,851 ; 18,152]	$\sqrt{2}\Delta x$
		2: [17,551 ; 18,451]	$3\Delta x$		2: [17,852 ; 18,151]	$\sqrt{2}\Delta x$
		3: [17,552 ; 18,151]	$\sqrt{5}\Delta x$			
		4: [17,851 ; 18,452]	$\sqrt{5}\Delta x$			
		5: [17,851 ; 18,751]	$3\Delta x$			
5	1028	1: [17,851 ; 18,152]	$\sqrt{2}\Delta x$	1011	1: [17,552 ; 18,151]	$\sqrt{5}\Delta x$
		2: [17,852 ; 18,151]	$\sqrt{2}\Delta x$		2: [17,851 ; 18,452]	$\sqrt{5}\Delta x$
6	1030	1: [17,852 ; 18,152]	Δx	1012	1: [17,852 ; 18,152]	Δx
7	1031	1: [17,551 ; 18,152]	$\sqrt{5}\Delta x$	1013	1: [17,251 ; 18,151]	$3\Delta x$
		2: [17,850 ; 18,152]	$\sqrt{5}\Delta x$		2: [17,851 ; 18,751]	$3\Delta x$
		3: [17,852 ; 18,150]	$\sqrt{5}\Delta x$			
		4: [17,852 ; 18,451]	$\sqrt{5}\Delta x$			
8	1032	1: [17,550 ; 18,152]	$2\sqrt{2}\Delta x$	1014	1: [17,551 ; 18,451]	$3\Delta x$
		2: [17,552 ; 18,152]	$2\Delta x$			
		3: [17,852 ; 18,450]	$2\sqrt{2}\Delta x$			
		4: [17,852 ; 18,452]	$2\Delta x$			
9	1033	1: [17,252 ; 18,152]	$3\Delta x$	1015	1: [17,551 ; 18,152]	$\sqrt{5}\Delta x$
	1033	2: [17,852 ; 18,752]	$3\Delta x$		2: [17,552 ; 18,152]	$2\Delta x$
					3: [17,852 ; 18,451]	$\sqrt{5}\Delta x$
					4: [17,852 ; 18,452]	$2\Delta x$
10	1034	1: [17,552 ; 18,452]	$3\Delta x$	1018	1: [17,850 ; 18,152]	$\sqrt{5}\Delta x$
		2: [17,553 ; 18,151]	$2\sqrt{2}\Delta x$		2: [17,852 ; 18,150]	$\sqrt{5}\Delta x$
		3: [17,553 ; 18,152]	$\sqrt{5}\Delta x$		3: [17,852 ; 18,153]	$\sqrt{2}\Delta x$
		4: [17,851 ; 18,453]	$2\sqrt{2}\Delta x$		4: [17,853 ; 18,152]	$\sqrt{2}\Delta x$
		5: [17,852 ; 18,453]	$\sqrt{5}\Delta x$			

TABLE 3. List of broken bonds and corresponding bond lengths for the first 10 stages of bond breaking, for the case of $\alpha = 2$, for the two bond-failure criteria in Example 2 (cf. Figures 6 and 7). Bonds are listed with the numbers of the pair of computational nodes they connect.

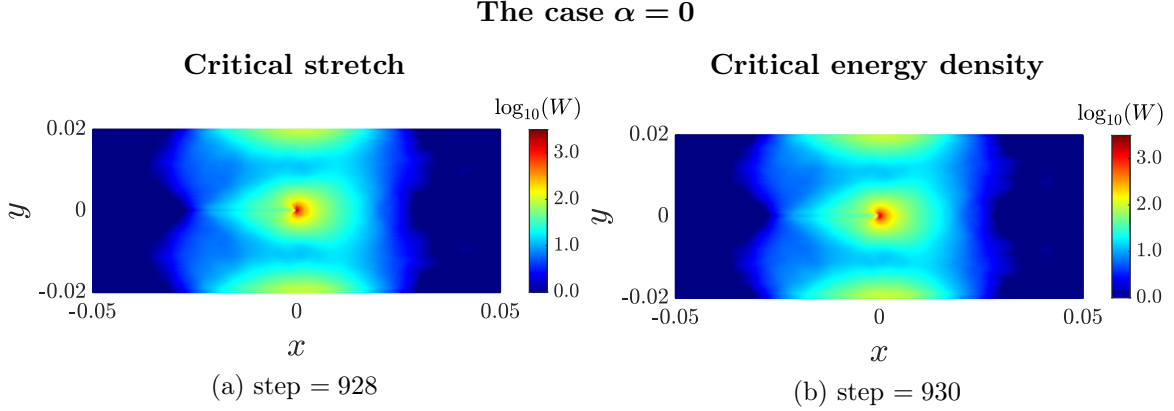


FIGURE 8. Comparison of the strain energy density field between the two bond-failure criteria at the time of initial bond breaking for $\alpha = 0$ in Example 2.

is a shortest bond of length Δx (see Table 3). This bond also breaks much earlier than the same one for the critical stretch criterion (step 1024; see Figure 6c), which only breaks after longer bonds (of length $\sqrt{5}\Delta x$; see Table 3) break. These longer bonds require more energy density to break for the critical energy density criterion, compared to the bond of length Δx , so they break second. We note that for both criteria, the same bonds break third, which are of length $2\Delta x$ (see Table 3 and Figures 6e and 6f). The fact that these bonds break in the same stage of bond breaking for both criteria is consistent with the fact that the same energy density is required for them to break in both criteria (*cf.* Figure 2b), even though they break at different time steps. Another example of shorter bonds breaking first for the critical energy density criterion is observed in the fourth stage of bond breaking (step 1010; see Figure 6h), where bonds of length $\sqrt{2}\Delta x$ (see Table 3) break at an early stage compared to the critical stretch criterion (step 1028; see Figure 6i), which only break after longer bonds (of length $\sqrt{5}\Delta x$ and $3\Delta x$; see Table 3) break.

A comparison of the strain energy density field at the time of initial bond breaking is provided in Figure 9. We observe that a larger amount of energy is required to initiate bond breaking under the critical stretch criterion (step 1022) compared to the critical energy density criterion (step 932).

5.3. Example 3: Crack propagation and branching. As in Section 5.2, we consider the problem of crack propagation in a pre-notched soda-lime glass thin plate subjected to traction loading [2]. In Section 5.2, we focused on the crack tip evolution by examining the initial stages of bond breaking that lead to crack propagation. Here, in contrast, we perform a full simulation and study the actual propagation of the crack.

The simulation employs a two-dimensional pre-notched rectangular plate under a plane stress assumption, with dimensions 0.1 m by 0.04 m, as illustrated in Figure 10. The material parameters are: mass density $\rho = 2,440 \text{ kg/m}^3$, Young's modulus $E = 72 \text{ GPa}$, and fracture energy $G_0 = 3.8 \text{ J/m}^2$; note that the thickness h is not used in the simulations because it does not appear in the equations in practice (see Remarks 2.3 and 4.1). The plate is initially at rest with zero initial displacements and velocities. We first consider in Section 5.3.1 the case of a lower traction, with a magnitude of $\sigma = 0.2 \text{ MPa}$ (as in Section 5.2), applied on the top and bottom of the plate. Then, in Section 5.3.2, we consider the case of a higher traction, with a magnitude of $\sigma = 2 \text{ MPa}$.

The case $\alpha = 2$

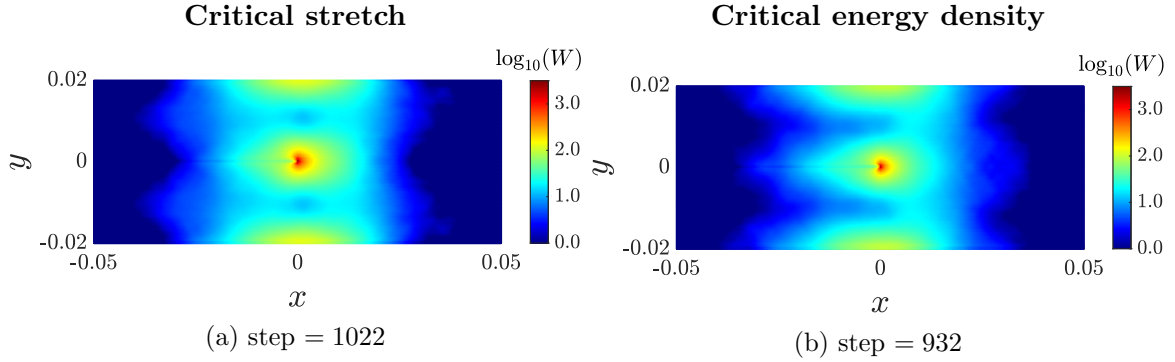


FIGURE 9. Comparison of the strain energy density field between the two bond-failure criteria at the time of initial bond breaking for $\alpha = 2$ in Example 2.

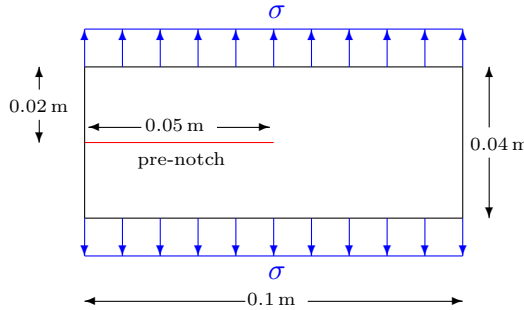


FIGURE 10. Illustration of the pre-notched thin plate under traction loading in Example 3.

The discretization employs the meshfree approach from [39] with a uniform grid of 300×120 computational nodes (total of 36,000 nodes) and a horizon of $\delta = 1 \times 10^{-3}$ m, which results in an m -ratio of $m = 3$ (*cf.* Figure 2a). The total simulation time is $T = 150 \mu\text{s}$, and the time step is $\Delta t = 67 \times 10^{-3} \mu\text{s}$. Time integration is performed via the velocity Verlet algorithm. In addition to the strain energy density field, the damage field introduced in [39] is computed. The computations employ the PDMATLAB2D code; see [36] for further details.

5.3.1. Lower traction: $\sigma = 0.2 \text{ MPa}$. In Figure 11, we compare the damage and strain energy density fields obtained using the critical stretch criterion (top plots) with those obtained using the critical energy density criterion (bottom plots) at the end of the simulation for the case of $\alpha = 0$. Although minor differences can be observed, especially in the strain energy density, overall the results are similar. To further assess the difference between the two criteria, we plot the evolution of the horizontal position of the crack tip over time. Note that, in Figure 11, the crack propagates horizontally for both criteria, so the vertical component of the crack tip position remains constant. To track the crack tip position over time, we select the right-most node with damage $\varphi > 0.35$ as the crack tip, see [12]. Figure 12a shows the results for the horizontal position of the crack tip over time for both criteria. The results suggest that crack propagation is initiated at the same time ($t \approx 74 \mu\text{s}$) for both criteria.

However, after the initial propagation, the crack tip of the critical stretch criterion simulation lags behind the crack tip of the critical energy density criterion simulation.

The case $\sigma = 0.2$ MPa and $\alpha = 0$

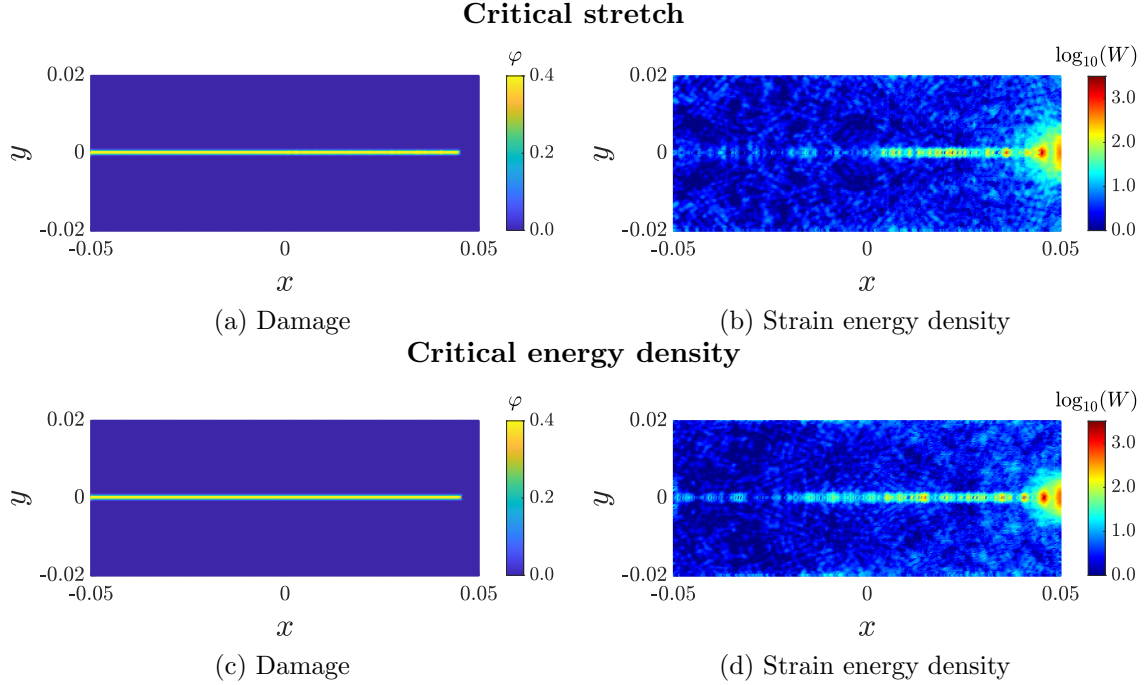


FIGURE 11. Comparison of the damage and strain energy density fields between the two bond-failure criteria for the case of $\sigma = 0.2$ MPa and $\alpha = 0$ at the final time in Example 3.

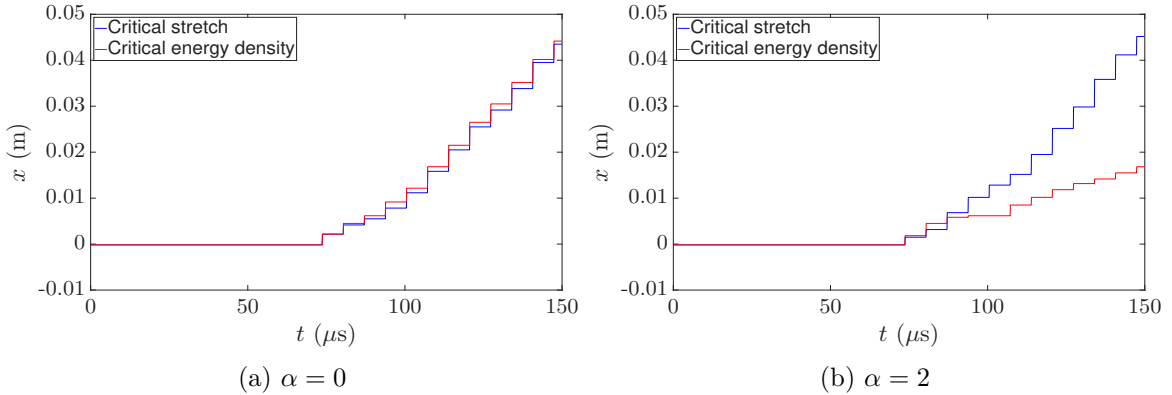


FIGURE 12. Comparison of the horizontal position of the crack tip over time between the two bond-failure criteria in Example 3.

In Figure 13, we compare the damage and strain energy density fields obtained using the critical stretch criterion (top plots) with those obtained using the critical energy density criterion (bottom plots) at the end of the simulation for the case of $\alpha = 2$. In this case, the difference between the two criteria is significant: for the critical stretch criterion, the crack

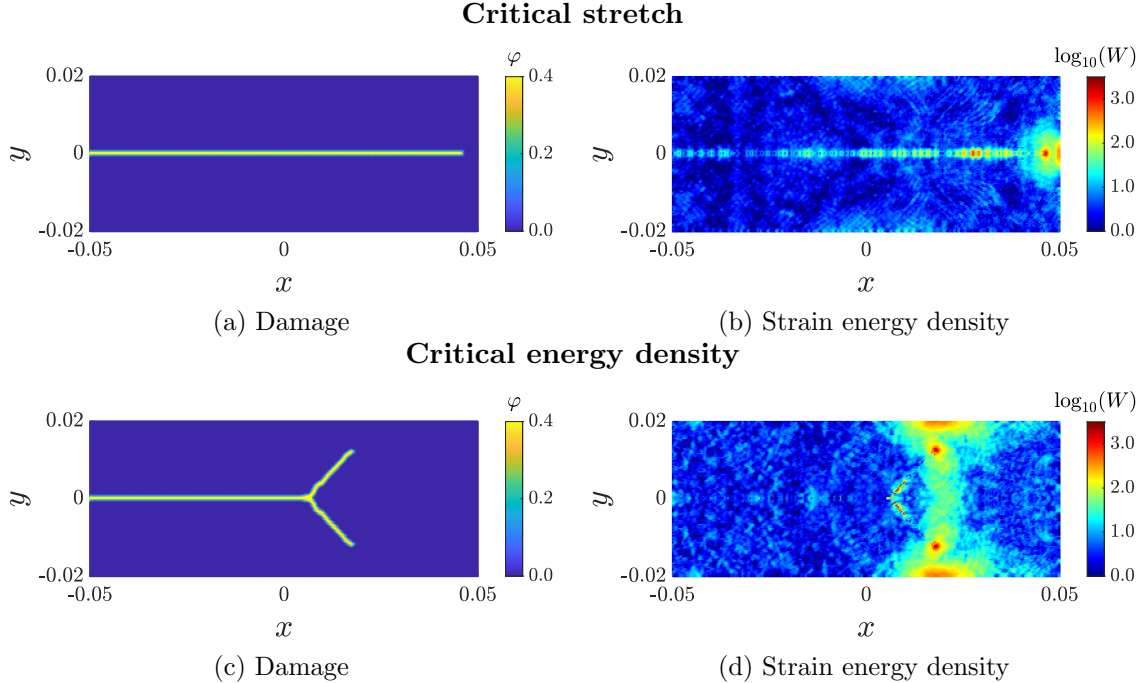
The case $\sigma = 0.2$ MPa and $\alpha = 2$ 

FIGURE 13. Comparison of the damage and strain energy density fields between the two bond-failure criteria for the case of $\sigma = 0.2$ MPa and $\alpha = 2$ at the final time in Example 3.

evolves as a single horizontal crack, whereas for the critical energy density criterion, the crack branches. We plot the horizontal position of the crack tip over time for both criteria in Figure 12b. Note that crack propagation is initiated at the same time for both criteria, which also coincides with the case of $\alpha = 0$ ($t \approx 74 \mu\text{s}$).

5.3.2. Higher traction: $\sigma = 2$ MPa. We now consider the case of traction with a tenfold magnitude, i.e., $\sigma = 2$ MPa. This case has been shown to lead to crack branching for the critical stretch criterion [2]. We run the same simulation as above, but with the new traction magnitude and a shorter simulation time of $T = 43 \mu\text{s}$. The results are shown in Figure 14 for $\alpha = 0$ and in Figure 15 for $\alpha = 2$. For $\alpha = 0$, small differences between the two bond-failure criteria are observed, especially in the strain energy density. For $\alpha = 2$, a more significant difference is observed in the resulting crack paths.

6. SUMMARY

This paper presented a mathematical analysis of the critical stretch and critical energy density bond-failure criteria for bond-based peridynamic fracture models. The analysis employed a model that generalizes the commonly used prototype microelastic brittle (PMB) constitutive model by incorporating an influence function. The critical energy density criterion was recast as a bond-dependent critical stretch criterion to rigorously prove that the two criteria are not equivalent in general and, consequently, result in different bond-breaking and fracture behaviors. In particular, depending on the choice of the influence function, certain bonds at critical stretch break under the critical stretch criterion but do not break under the

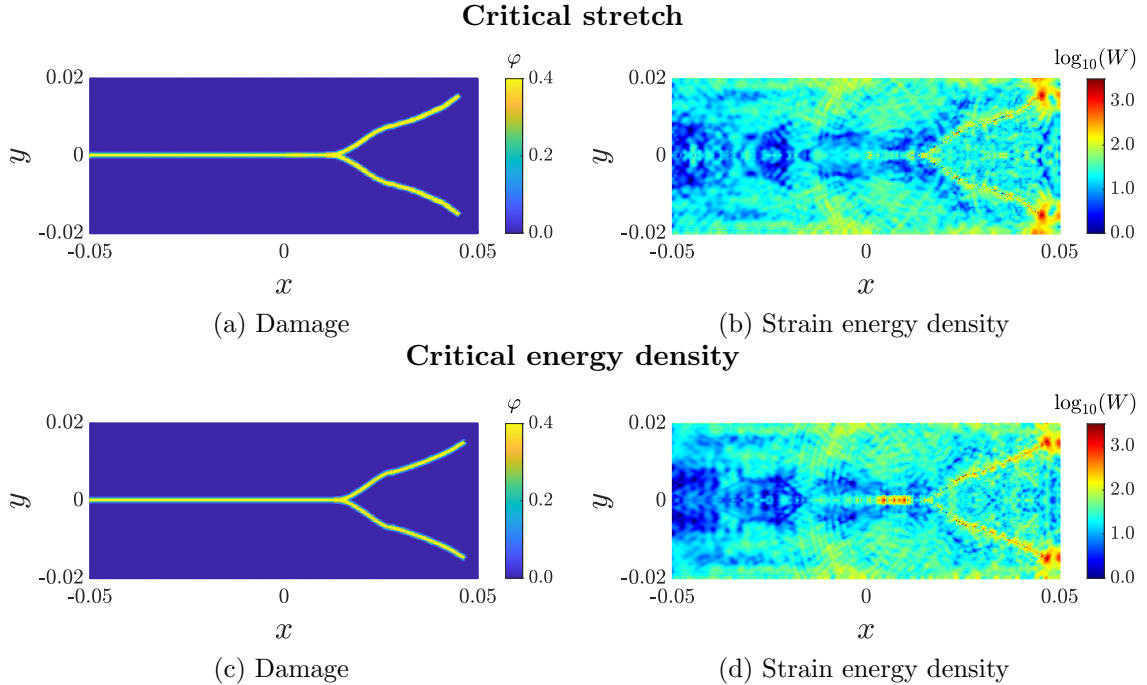
The case $\sigma = 2$ MPa and $\alpha = 0$ 

FIGURE 14. Comparison of the damage and strain energy density fields between the two bond-failure criteria for the case of $\sigma = 2$ MPa and $\alpha = 0$ at the final time in Example 3.

critical energy density criterion, and vice versa. Moreover, for the critical energy density criterion, the choice of influence function may dictate whether shorter or longer bonds break first; this behavior is absent in the critical stretch criterion. Additionally, we prove that the two bond-failure criteria are equivalent if and only if the influence function is $\omega(\|\xi\|) = \beta\|\xi\|^{-1}$ for some $\beta > 0$. Our findings were confirmed numerically for two-dimensional problems, with examples presented for isotropic extension, crack tip evolution, and crack branching. It was revealed that the speed at which the crack tip evolves and the branching effect depend heavily on both the bond-failure criterion and the influence function.

7. ACKNOWLEDGEMENTS

P. Seleson was supported by the Laboratory Directed Research and Development Program of Oak Ridge National Laboratory, managed by UT-Battelle, LLC, for the U. S. Department of Energy. P. R. Stinga was supported by Simons Foundation grant MP-TSM-00002709.

REFERENCES

- [1] A. R. Aguiar, T. V. B. Patriota, Brittle fracture modeling using ordinary state-based peridynamics with continuous bond-breakage damage, *J. Peridyn. Nonlocal Model.* **5** (2023), 81–120.
- [2] F. Bobaru, G. Zhang, Why do cracks branch? A peridynamic investigation of dynamic brittle fracture, *Int. J. Fract.* **196** (2015), 59–98.
- [3] V. Diana and S. Casolo, A bond-based micropolar peridynamic model with shear deformability: Elasticity, failure properties and initial yield domains, *Int. J. Solids Struct.* **160** (2019), 201–231.
- [4] D. Dipasquale, G. Sarego, P. Prapamonthon, S. Yooyen, and A. Shojaei, A stress tensor-based failure criterion for ordinary state-based peridynamic models, *J. Appl. Comput. Mech.* **8** (2022), 617–628.

The case $\sigma = 2$ MPa and $\alpha = 2$

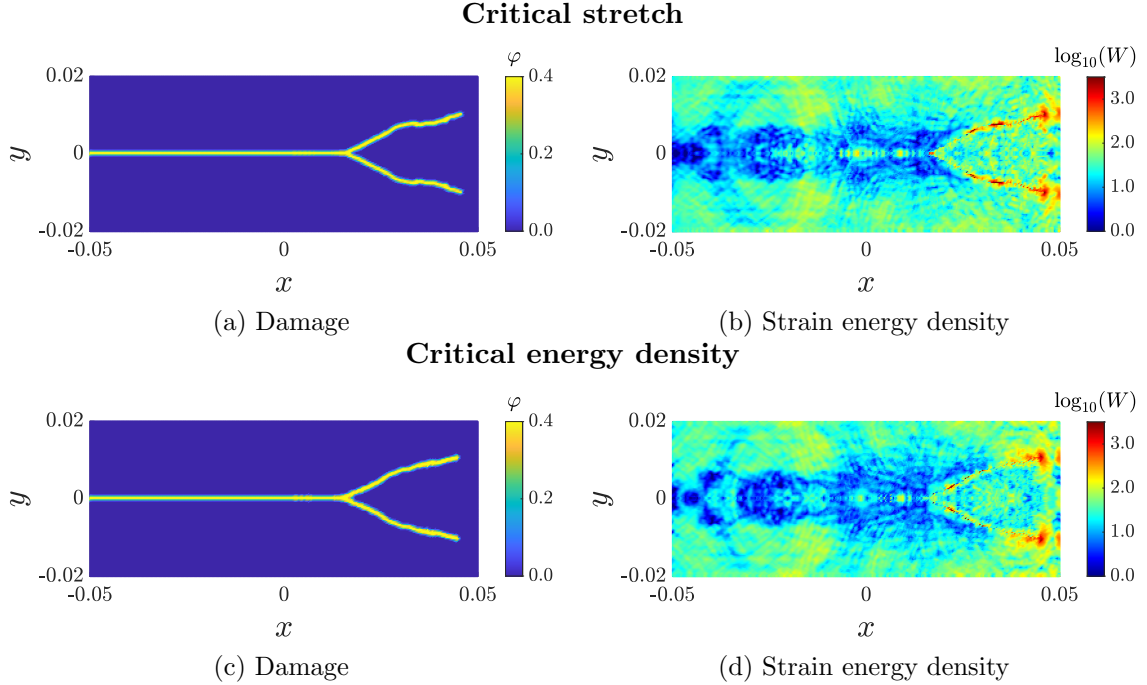


FIGURE 15. Comparison of the damage and strain energy density fields between the two bond-failure criteria for the case of $\sigma = 2$ MPa and $\alpha = 2$ at the final time in Example 3.

- [5] D. Dipasquale, G. Sarego, M. Zaccariotto, and U. Galvanetto, A discussion on failure criteria for ordinary state-based peridynamics, *Eng. Fract. Mech.* **186** (2017), 378–398.
- [6] Q. Du, Y. Tao, and X. Tian, A peridynamic model of fracture mechanics with bond-breaking, *J. Elasticity* **132** (2018), 197–218.
- [7] E. Emmrich and D. Puhst, A short note on modeling damage in peridynamics, *J. Elasticity* **123** (2016), 245–252.
- [8] J. T. Foster, S. A. Silling, and W. Chen, An energy based criterion for use with peridynamic states, *Int. J. Multiscale Comput. Eng.* **9** (2011), 675–687.
- [9] W. Gerstle, N. Sau, and S. Silling, Peridynamic modeling of concrete structures, *Nucl. Eng. Des.* **237** (2007), 1250–1258.
- [10] W. Gerstle, N. Sau, and S. Silling, Peridynamic modeling of plain and reinforced concrete structures, *In: 18th International Conference on Structural Mechanics in Reactor Technology (SMiRT 18)*, (2005), 54–68.
- [11] M. Ghajari, L. Iannucci, and P. Curtis, A peridynamic material model for the analysis of dynamic crack propagation in orthotropic media, *Comput. Methods Appl. Mech. Engrg.* **276** (2014), 431–452.
- [12] Y. D. Ha, F. Bobaru, Studies of dynamic crack propagation and crack branching with peridynamics, *Int. J. Fract.* **162** (2010), 229–244.
- [13] G. Hattori, J. Trevelyan, and W. M. Coombs, A non-ordinary state-based peridynamics framework for anisotropic materials, *Comput. Methods Appl. Mech. Engrg.*, **339** (2018), 416–442.
- [14] M. Ignatiev, N. Kazarinov, and Y. Petrov, Peridynamic modelling of the dynamic crack initiation, *Procedia Struct. Integr.*, **28** (2020), 1650–1654.
- [15] M. Ignatiev and E. Oterkus, Remote stress fracture criterion in peridynamics, *Engineering with Computers*, **41** (2025), 3169–3192.
- [16] M. O. Ignatiev, Y. V. Petrov, and N. A. Kazarinov, Simulation of dynamic crack initiation based on the peridynamic numerical model and the incubation time criterion, *Tech. Phys.*, **66**(3) (2021), 422–425.

- [17] M. O. Ignatiev, Y. V. Petrov, N. A. Kazarinov, and E. Oterkus, Peridynamic formulation of the mean stress and incubation time fracture criteria and its correspondence to the classical Griffith's approach, *Continuum Mech. Thermodyn.*, **35** (2023), 1523–1534.
- [18] O. Karpenko, S. Oterkus, and E. Oterkus, An in-depth investigation of critical stretch based failure criterion in ordinary state-based peridynamics, *Int. J. Fract.* **226** (2020), 97–119.
- [19] W.-J. Li, Q.-Z. Zhu, Y.-L. Du, and J.-F. Shao, An extended bond-based peridynamic model with bond transverse deformation effects for quasi-brittle rocks, *Int. J. Rock Mech. Min. Sci.*, **190** (2025), 106099.
- [20] R. Lipton, Cohesive dynamics and brittle fracture, *J. Elasticity* **124** (2016), 143–191.
- [21] R. Lipton, Dynamic brittle fracture as a small horizon limit of peridynamics, *J. Elasticity*, **117** (2014), 21–50.
- [22] R. Lipton, E. Said, and P. Jha, Free damage propagation with memory, *J. Elasticity* **133** (2018), 129–153.
- [23] W. K. Liu, S. Li, and H. S. Park, Eighty years of the finite element method: birth, evolution, and future, *Arch. Comput. Methods Eng.* **29** (2022), 4431–4453.
- [24] E. Madenci, A. Barut, and N. Phan, Bond-based peridynamics with stretch and rotation kinematics for opening and shearing modes of fracture, *J. Peridyn. Nonlocal Model.*, **3** (2021), 211–254.
- [25] E. Madenci and S. Oterkus, Ordinary state-based peridynamics for plastic deformation according to von Mises yield criteria with isotropic hardening, *J. Mech. Phys. Solids* **86** (2016), 192–219.
- [26] E. Madenci and E. Oterkus, Peridynamic Theory and Its Applications, Springer, New York, 2014.
- [27] J. O'Grady and J. Foster, Peridynamic beams: A non-ordinary, state-based model, *Int. J. Solids Struct.* **51** (2014): 3177–3183.
- [28] E. Oterkus and E. Madenci, Peridynamic analysis of fiber-reinforced composite materials, *J. Mech. Mater. Struct.* **7** (2012), 45–84.
- [29] S. Oterkus and E. Madenci, Peridynamics for antiplane shear and torsional deformations, *J. Mech. Mater. Struct.* **10**(2) (2015), 167–193.
- [30] K. Ravi-Chandar and W. G. Knauss, An experimental investigation into dynamic fracture: IV. On the interaction of stress waves with propagating cracks, *Int. J. Fract.* **26** (1984), 189–200.
- [31] B. Ren, C. T. Wu, P. Seleson, D. Zeng, and D. Lyu, A peridynamic failure analysis of fiber-reinforced composite laminates using finite element discontinuous Galerkin approximations, *Int. J. Fract.* **214** (2018), 49–68.
- [32] B. Ren, C. T. Wu, P. Seleson, D. Zeng, M. Nishi, and M. Pasetto, An FEM-based peridynamic model for failure analysis of unidirectional fiber-reinforced laminates, *J. Peridyn. Nonlocal Model.* **4** (2022), 139–158.
- [33] H. Ren, X. Zhuang, and T. Rabczuk, A new peridynamic formulation with shear deformation for elastic solid, *J. Micromech. Mol. Phys.* **1** (2016), 1650016.
- [34] P. D. Seleson, Peridynamic multiscale models for the mechanics of materials: constitutive relations, up-scaling from atomistic systems, and interface problems, Thesis (Ph.D.)-The Florida State University (2010), 143pp.
- [35] P. Seleson and M. Parks, On the role of the influence function in the peridynamic theory, *Int. J. Multiscale Comput. Eng.* **9** (2011), 689–706.
- [36] P. Seleson, M. Pasetto, Y. John, J. Trageser, and S. Temple Reeve, PDMATLAB2D: a peridynamics MATLAB two-dimensional code, *J. Peridyn. Nonlocal Model.* **6** (2024), 149–205.
- [37] Y. Shou, X. Zhou, and F. Berto, 3D numerical simulation of initiation, propagation and coalescence of cracks using the extended non-ordinary state-based peridynamics, *Theoretical and Applied Fracture Mechanics* **101** (2019) ,254–268
- [38] S. A. Silling, Reformulation of elasticity theory for discontinuities and long-range forces, *J. Mech. Phys. Solids* **48** (2000), 175–209.
- [39] S. A. Silling and E. Askari, A meshfree method based on the peridynamic model of solid mechanics, *Comput. Struct.* **83** (2005), 1526–1535.
- [40] S. A. Silling, M. Epton, O. Weckner, J. Xu, and E. Askari, Peridynamic states and constitutive modeling, *J. Elasticity* **88** (2007), 151–184.
- [41] S. A. Silling and R. B. Lehoucq, Convergence of peridynamics to classical elasticity theory, *J. Elasticity*, **93** (2008), 13–37.
- [42] Z. Song, G. Wang, D. Lu, X. Zhou, T. Rabczuk, and X. Du, A modeling method of failure for concrete considering the stress state in peridynamics, *Int. J. Solids Struct.*, **320** (2025), 113536.
- [43] J. Trageser and P. Seleson, Bond-based peridynamics: a tale of two Poisson's ratios, *J. Peridyn. Nonlocal Model.*, **2** (2020), 278–288.

- [44] M. R. Tupek, J. J. Rimoli, and R. Radovitzky, An approach for incorporating classical continuum damage models in state-based peridynamics, *Comput. Methods Appl. Mech. Engrg.* **263** (2013), 20–26.
- [45] Y. Wang, X. Zhou, Y. Wang, and Y. Shou, A 3-D conjugated bond-pair-based peridynamic formulation for initiation and propagation of cracks in brittle solids, *Int. J. Solids Struct.*, **134** (2018), 89–115.
- [46] W. Wang, Q.-Z. Zhu, T. Ni, B. Vazic, P. Newell, and S. P. A. Bordas, An extended peridynamic model equipped with a new bond-breakage criterion for mixed-mode fracture in rock-like materials, *Comput. Methods Appl. Mech. Engrg.* **411** (2023), 116016.
- [47] T. L. Warren, S. A. Silling, A. Askari, O. Weckner, M. A. Epton, and J. Xu, A non-ordinary state-based peridynamic method to model solid material deformation and fracture, *Int. J. Solids Struct.*, **46** (2009), 1186–1195.
- [48] Z. Yang, H. Wang, and M. Sharma, A peridynamic compensated critical energy density criterion for mixed-mode fracturing in quasi-brittle materials, *Theor. Appl. Fract. Mech.*, **134** (2024), 104736.
- [49] Y. Zhang and P. Qiao, A new bond failure criterion for ordinary state-based peridynamic mode II fracture analysis, *Int. J. Fract.* **215** (2019), 105–128.
- [50] H. Zhang and P. Qiao, A state-based peridynamic model for quantitative fracture analysis, *Int. J. Fract.* **211** (2018), 217–235.
- [51] X.-P. Zhou and Y.-T. Wang, Numerical simulation of crack propagation and coalescence in pre-cracked rock-like Brazilian disks using the non-ordinary state-based peridynamics, *Int. J. Rock Mech. Min. Sci.*, **89** (2016), 235–249.

(P. Seleson) COMPUTER SCIENCE AND MATHEMATICS DIVISION, OAK RIDGE NATIONAL LABORATORY, P.O. Box 2008, MS-6013, OAK RIDGE, TN 37831, USA

Email address: selesonpd@ornl.gov

(P. R. Stinga) DEPARTMENT OF MATHEMATICS, IOWA STATE UNIVERSITY, 396 CARVER HALL, AMES, IA 50011, USA

Email address: stinga@iastate.edu

(M. Vaughan) DEPARTMENT OF MATHEMATICS, TEXAS STATE UNIVERSITY, MCS 470, SAN MARCOS, TX 78666, USA

Email address: vaughan@txstate.edu